References

1. Nakabeppu Y, Tominaga Y, Tsuchimoto D, et al. Mechanisms protecting genomic integrity from damage caused by reactive oxygen species: implications for carcinogenesis and neurodegeneration. Environ Mutagen Res. 2001;23:183-195.
2. Friedberg EC, Walker GC, Siede W. DNA Repair and Mutagenesis. Washington, DC: American Society for Microbiology; 1995.
3. Parker A, Gu Y, Mahoney W, Lee SH, Singh KK, Lu AL. Human homolog of the MutY repair protein (hMYH) physically interacts with proteins involved in long patch DNA base excision repair. J Biol Chem. 2001;276:5547-5555.
4. Otterlei M, Warbrick E, Nagelhus TA, et al. Post-replicative base excision repair in replication foci. EMBO J. 1999;18:3834-3844.
5. Hayashi H, Tominaga Y, Hirano S, McKenna AE, Nakabeppu Y, Matsumoto Y. Replication-associated repair of adenine:8-oxoguanine mispairs by MYH. Curr Biol. 2002;12:335-339.
6. Nilsen H, Rosewell I, Robins P, et al. Uracil-DNA glycosylase (UNG)-deficient mice reveal a primary role of the enzyme during DNA replication. Mol Cell. 2000;5:1059-1065.
7. Seki S, Ikeda S, Watanabe S, et al. A mouse DNA repair enzyme (APEX nuclease) having exonuclease and apurinic/apyrimidinic endonuclease activities: purification and characterization. Biochim Biophys Acta. 1991;1079:57-64.
8. Hadi MZ, Wilson DM 3rd. Second human protein with homology to the Escherichia coli abasic endonuclease exonuclease III. Environ Mol Mutagen. 2000;36:312-324.
9. Tsuchimoto D, Sakai Y, Sakumi K, et al. Human APE2 protein is mostly localized in the nuclei and to some extent in the mitochondria, while nuclear APE2 is partly associated with proliferating cell nuclear antigen. Nucleic Acids Res. 2001;29:2349-2360.
10. Demple B, Herman T, Chen DS. Cloning and expression of APE, the cDNA encoding the major human apurinic endonuclease: definition of a family of DNA repair enzymes. Proc Natl Acad Sci U S A. 1991;88:11450-11454.
11. Robson CN, Hickson ID. Isolation of cDNA clones encoding a human apurinic/apyrimidinic endonuclease that corrects DNA repair and mutagenesis defects in E. coli xth (exonuclease III) mutants. Nucleic Acids Res. 1991;19:5519-5523.
12. Xanthoudakis S, Curran T. Identification and characterization of Ref-1, a nuclear protein that facilitates AP-1 DNA-binding activity. EMBO J. 1992;11:653-665.
13. Xanthoudakis S, Smeyne RJ, Wallace JD, Curran T. The redox/DNA repair protein, Ref-1, is essential for early embryonic development in mice. Proc Natl Acad Sci U S A. 1996;93:8919-8923.
14. Ide Y, Tsuchimoto D, Tominaga Y, Iwamoto Y, Nakabeppu Y. Characterization of the genomic structure and expression of the mouse Apex2 gene. Genomics. 2003;81:47-57.
15. Oda S, Nishida J, Nakabeppu Y, Sekiguchi M. Stabilization of cyclin E and cdk2 mRNAs at G1/S transition in Rat-1A cells emerging from the G0 state. Oncogene. 1995;10:1343-1351.
16. Vergani C, Stabilini R, Agostoni A. Quantitative determination of serum immunoglobulins by single radial immunodiffusion on cellulose acetate. Immunochemistry. 1967;4:233-237.
17. Ernst B, Surh CD, Sprent J. Thymic selection and cell division. J Exp Med. 1995;182:961-971.
18. Rada C, Williams GT, Nilsen H, Barnes DE, Lindahl T, Neuberger MS. Immunoglobulin isotype switching is inhibited and somatic hypermutation perturbed in UNG-deficient mice. Curr Biol. 2002;12:1748-1755.
19. Imai K, Slupphaug G, Lee WI, et al. Human uracil-DNA glycosylase deficiency associated with profoundly impaired immunoglobulin class-switch recombination. Nat Immunol. 2003;4:1023-1028.
20. Nilsen H, Stamp G, Andersen S, et al. Gene-targeted mice lacking the Ung uracil-DNA glycosylase develop B-cell lymphomas. Oncogene. 2003;22:5381-5386.
21. Nishioka K, Ohtsubo T, Oda H, et al. Expression and differential intracellular localization of two major forms of human 8-oxoguanine DNA glycosylase encoded by alternatively spliced OGG1 mRNAs. Mol Biol Cell. 1999;10:1637-1652.
22. Ohtsubo T, Nishioka K, Imaiso Y, et al. Identification of human MutY homolog (hMYH) as a repair enzyme for 2-hydroxyadenine in DNA and detection of multiple forms of hMYH located in nuclei and mitochondria. Nucleic Acids Res. 2000;28:1355-1364.
23. Morland I, Rolseth V, Luna L, Rognes T, Bjoras M, Seeberg E. Human DNA glycosylases of the bacterial Fpg/MutM superfamily: an alternative pathway for the repair of 8-oxoguanine and other oxidation products in DNA. Nucleic Acids Res. 2002;30:4926-4936.
24. Johnson RE, Torres-Ramos CA, Izumi T, Mitra S, Prakash S, Prakash L. Identification of APN2, the Saccharomyces cerevisiae homolog of the major human AP endonuclease HAP1, and its role in the repair of abasic sites. Genes Dev. 1998;12:3137-3143.
25. Guillet M, Boiteux S. Origin of endogenous DNA abasic sites in Saccharomyces cerevisiae. Mol Cell Biol. 2003;23:8386-8394.

Neuropathology 2004; **24**, 125–130

Original Article

Defense mechanism to oxidative DNA damage in glial cells

Takashi Iida,[1,3] Akiko Furuta,[1,3] Yusaku Nakabeppu[2,3] and Toru Iwaki[1,3]

[1]Department of Neuropathology, Neurological Institute, Graduate School of Medical Sciences, [2]Division of Neurofunctional Genomics, Medical Institute of Bioregulation, Kyushu University, Fukuoka and [3]CREST, Japan Science and Technology Corporation, Tokyo, Japan.

Astrocytosis is a sequential morphological change of astrocytic reaction to tissue damage, and is associated with regulation of antioxidant defense mechanisms to reduce oxidative damage. The repair enzymes to oxidative DNA damage, oxidized purine-nucleoside triphosphatase (hMTH1) and a mitochondrial type of 8-oxoguanine DNA glycosylase (hOGG1–2a) in brain tumors and neurons of Alzheimer's disease, were previously reported. In the present study, glial expression of these repair enzymes under such pathological conditions as cerebrovascular diseases and metastatic brain tumors, were investigated. Furthermore, an *in-vitro* experiment using a glioma cell-line under oxidative stress was performed to verify the immunohistochemical results of post-mortem materials. As a result, hOGG1–2a immunoreactivities in reactive astrocytes were more intense than those to hMTH1. Oligodendrocytes of acute or subacute stage of brain infarction were strongly immunoreactive to both repair enzymes. *In-vitro* study revealed that, hOGG1–2a is constitutively expressed in both untreated glioma cells and the glioma cells under oxidative stress. However, although no immunoreactivity to hMTH1 was found in the control cells, accumulation of hMTH1 was rapidly induced by oxidative stress. These results indicate that the two repair enzymes to oxidative DNA damage are differentially regulated in glial cells, and that there is a difference in the expression of the repair enzymes between reactive astrocytes and oligodendrocytes.

Key words: 8-oxoguanine DNA glycosylase, astrocytes, oligodendrocyte, oxidative stress, oxidized purine-nucleoside triphosphatase.

Correspondence: Toru Iwaki, MD, Department of Neuropathology, Neurological Institute, Graduate School of Medical Sciences, Kyushu University, Fukuoka, 812-8582, Japan. Email: iwaki@np.med.kyushu-u.ac.jp

Received and revised 14 July 2003; accepted 6 October 2003.

INTRODUCTION

Astrocytosis is a sequential morphological change of astrocytic reaction to tissue damage. The neuroprotective role of astrocytes to oxidative stress has been previously reported,[1–3] and appears most evident following reactive gliosis.[3] Manganaro *et al.* reported that the cytoprotective responses to cysteamine-related oxidative stress in astrocytes facilitated astrocyte survival and the development of reactive gliosis in the face of concomitant neuronal degeneration.[1] Reactive astrocytes are also characterized by up-regulation of astrocytic antioxidants such as metallothioneins in an animal model of epilepsy and in human degenerative diseases.[3,4] Astrocytes also respond to prolonged oxidative stress by up-regulating plasma membrane cystine transport activity, using the acquired amino acid for glutathione synthesis, and increasing their glutathione content.[5] In addition, the relationship between oxidative stress and oligodendrocytes has also been frequently reported.[6–11]

An oxidized form of guanine, 8-Oxoguanine, causes A:T to C:G or G:C to T:A transversion mutations, because of its base pairing nature with adenine as well as cytosine.[12] Organisms are equipped with protective mechanisms to avoid such errors in DNA caused by 8-oxoguanine.[12–14] The human *OGG1* gene encodes an 8-oxoguanine DNA glycosylase (hOGG1), which removes 8-oxoguanine paired with cytosine, and one of the seven spliced forms, type 2a (hOGG1–2a), is frequently found in human tissues including the brain.[15] Human oxidized purine nucleoside triphosphatase (hMTH1) protein hydrolyzes oxidized purine-nucleoside triphosphates to the corresponding monophosphate, thereby preventing misincorporation of 8-oxo-dG into DNA.[12,16–18] Therefore we used antibodies against hOGG1–2a and hMTH1 to investigate brain tumors and Alzheimer's disease.[19–21]

We found the expression of hOGG1–2a was shown in reactive astrocytes in Alzheimer's disease,[21] as well as that of superoxide dismutase,[22] and considered that DNA

repair enzymes might also be up-regulated in reactive astrocytes like the antioxidant enzymes.[3] Except for the report by Iida *et al.*,[21] previous studies about oxidative DNA damage in the brain were mainly regarding the neuron; few studies about oxidative DNA damage in astrocytes or oligodendrocytes that support the neuron have been done. In the present study, we focused on perilesional expression of the repair enzymes to oxidative DNA damage in glial cells. To evaluate the expression of the repair enzymes, we investigated immunohistochemistry of postmortem human brain tissues. We selected mainly cases of metastatic brain tumors and cerebrovascular diseases, which are common diseases of the brain that are accompanied with astrocytosis. Furthermore, *in-vitro* experiment using a glioma cell-line under oxidative stress was performed to verify the immunohistochemical results of postmortem materials.

MATERIALS AND METHODS

Immunohistochemistry of human post-mortem materials

Tissues were obtained from autopsied cases (Table 1) consisting of 10 men and five women bearing eight metastatic brain tumors and seven brain infarcts. The histology of all the metastatic brain tumors was adenocarcinoma.

The following antibodies were used in the present study. A rabbit polyclonal antibody (0.5 μg/mL) against hMTH1 protein (anti-MTH1) was raised by immunizing the recombinant hMTH1d protein, and were affinity-purified by the aid of antigen-columns.[23,24] A rabbit polyclonal antibody (anti2a-CT) recognizing the mitochondrial form of hOGG1 (hOGG1–2a) was raised against fusion proteins containing the amino acid sequence of C-terminus of hOGG1–2a and affinity-purified.[15] Immunohistochemistry with anti-MTH1, anti-hOGG1–2a, anti-GFAP (mouse monoclonal antibody, 1:100 dilution, clone GA5; Novacastra, Newcastle upon Tyne, UK) was performed on paraffin sections by the indirect immunoperoxidase method.

The specimens were fixed in 10% formalin, embedded in paraffin and then sectioned at 7 μm thickness. The sections were deparaffinized in xylene and hydrated in an ethanol gradient. The endogenous peroxidase activity was blocked with 0.3% H_2O_2 in absolute methanol for 30 min at room temperature. After being rinsed in tap water, the sections were completely immersed in citrate buffer and then autoclaved for 10 min for immunohistochemical analysis of hMTH1. The sections were then washed in 50 mmol/L Tris-HCl (pH 7.6), followed by overnight incubation with the primary antibodies at 4°C. After being washed in the same buffer, the sections were incubated with horseradish peroxidase-conjugated secondary antibody (1:200 dilution; Vector Laboratories, Burlingame, CA, USA). The colored reaction product was developed with 3,3′-diaminobenzidine tetrahydrochloride solution. Immunohistochemical procedures were performed in the same condition with respect to the incubation time. Expression of hMTH1 and hOGG1–2a is scored as follows: (–) all of

Table 1 Immunohistochemistry of human autopsied materials

Case no.	Age	Sex	Diagnosis	Location	Clinical duration	Astrocytosis	IR of astrocytes		IR of oligodendrocytes	
							hMTH1	hOGG1–2a	hMTH1	hOGG1–2a
A. Metastatic brain tumors										
1	54	M	Lung	Cerebrum		++	+	++(n)	+	+
2	28	F	Lung	Cerebellum		++	++	+(n)	+	±
3	74	F	Lung	Cerebrum		++	±	++(n)	±	±
4	59	M	Lung	Cerebellum		++	–	+(n)	–	±
5	85	F	Thyroid	Cerebrum		++	+	++(n)	+	+
6	65	M	Stomach	Cerebrum		++	+	++(n)	–	±
7	71	M	Lung	Cerebrum		++	±	+(n)	+	+
8	31	F	Breast	Cerebrum		++	–	++(n)	+	–
B. Brain infarcts										
9	79	M	Infarct	Medulla	8 hours	+	+	+	++	+
10	84	M	Infarct	Cerebrum	24 days	++	+	++(n)	+	+
11	79	F	Infarct	Thalamus	1 months	++	–	+	±	+
12	88	M	Infarct	Pons	1 months	++	±	+	±	+
13	39	M	Infarct	Cerebrum	5 months	++	±	++(n)	±	++
14	75	M	Infarct	Cerebrum	28 months	++	±	+(n)	+	±
15	70	M	Infarct	Thalamus	48 months	–	–	–	±	±

IR, immunoreactivity; hMTH1, oxidized purine-nucleoside triphosphatase; hOGG1–2a, a mitochondrial type of 8-oxoguanine DNA glycosylase; M, male; F, female; (n), the existence of nuclear staining in addition to cytoplasm. Expression of hMTH1 and hOGG1–2a is scored as follows: (–), all reactive astrocytes/oligodendroglial cells around the lesion are negative; (±), less than 5% are positive (fainlty positive); (+), 5–50% of the cell are positive; (++), more than 50% cells are positive (strongly positive); (++), astrocytosis is significant (+), astrocytosis is not significant; (–), astrocytosis is undetectable.

the perilesional reactive astrocytes/oligodendroglial cells are negative; (+/–) less than 5% of cells are positive (faintly positive); (+) 5–50% of cells are positive; (+ +) more than 50% of cells are positive (strongly positive). Astrocytosis was identified by immunostaining of GFAP.

Cell culture under oxidative stress

We used a human glioma cell line (KNS81).[25] KNS81 was cultivated in Dulbecco's modified Eagles' medium/Ham's F-12 with a mixture of 1:1 (Sigma, St.Louis, MO, USA) containing 10% fetal bovine serum. Oxidative stress was administrated by exposing cells to 10 mmol/L and 20 mmol/L H_2O_2 with serum-free medium for 30 min After the treatment, the medium was changed to a fresh one, and cells were maintained for 16 h at 37°C.

Indirect immunocytochemistry was performed for the culture study. The glioma cells were fixed with 10% buffered formalin in PBS for 30 min, rinsed in PBS, and treated with 0.1% Nonidet P-40 in PBS for 10 min. After being washed in PBS, the cells were then incubated sequentially with anti-hMTH1 or anti-hOGG1–2a antibody at 4°C overnight. After being washed in PBS, the sections were incubated with horseradish peroxidase-conjugated secondary antibody. The colored reaction product was developed with 3,3′-diaminobenzidine tetrahydrochloride solution. The sections were counterstained lightly with HE.

RESULTS

Immunohistochemistry of human post-mortem materials hOGG1–2a was faintly expressed in neuronal cytoplasm and astrocytes, while significant immunoreactivity for hMTH1 was not detectable in the cerebral cortex (Fig. 1). The immunohistochemical results of pathological conditions were summerized in Table 1.

Metastatic tumors

With regard to hOGG1–2a expression in reactive astrocytes, all eight cases were graded as positive or strongly positive, while four cases were graded as positive and the other four cases were graded as negative or faintly positive in hMTH1 expression. A representative profile of the immunohistochemistry is shown in Fig. 2. Reactive astrocytosis was present around the metastatic adenocarcinoma and hOGG1–2a was strongly expressed in the reactive astrocytes. Human oxidized purine nucleoside triphosphatase was strongly expressed in the adenocarcinoma cells, but not in the reactive astrocytes. All eight cases showed nuclear staining of hOGG1–2a in the reactive astrocytes in addition to the cytoplasmic staining. In some cases, nuclear staining was more conspicuous than cytoplasmic staining in reactive astrocytes.

Brain infarcts

The locations of brain infarcts were various as shown in Table 1. A representative profile of the immunohistochemistry is shown in Fig. 3. With regard to hOGG1–2a expression in reactive astrocytes, six cases were graded as positive or strongly positive, while two cases were graded as positive and the other five cases were graded as negative or faintly positive in hMTH1 expression. Three cases showed nuclear and cytoplasmic immunoreactivities to hOGG1–2a antibody in reactive astrocytes. With regard to hOGG1–2a expression in oligodendrocytes, five cases were graded as negative or faintly positive, the other three cases were graded as positive. Five cases were graded as positive and the other three cases were graded as negative or faintly positive in hMTH1 expression.

In summary, immunoreactivities for hOGG1–2a in reactive astrocytes were usually strongly positive, while those for hMTH1 were negative or faintly positive. Positive

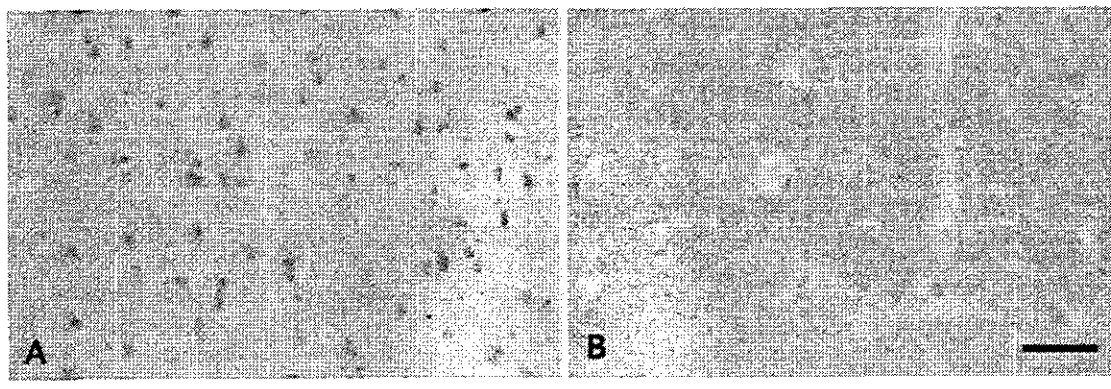

Fig. 1 Immunohistochemistry for a mitochondrial type of 8-oxoguanine DNA glycosylase (hOGG1–2a) and oxidized purine-nucleoside triphosphatase (hMTH1) in normal cerebral cortex. (A), hOGG1–2a is faintly expressed in neuronal cytoplasm and astrocytes; (B), no hMTH1 expression is seen in the cerebral cortex . (A,B), bar = 50 μm.

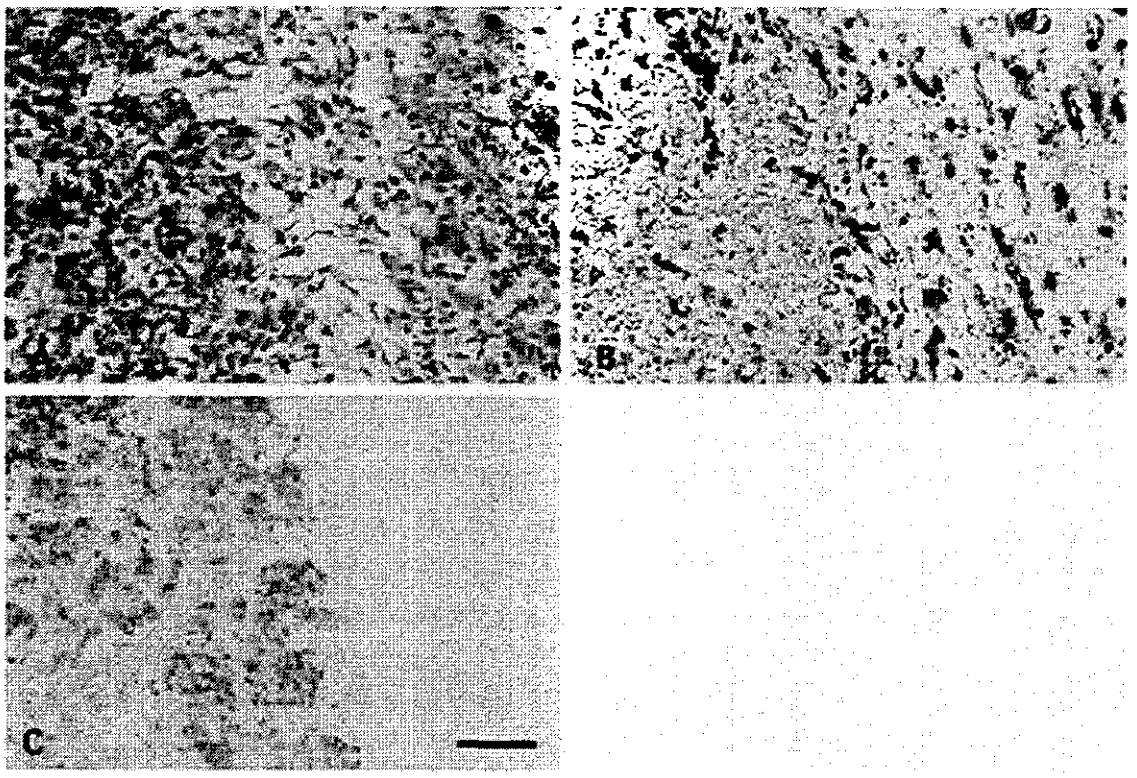

Fig. 2 Immunohistochemistry of metastatic brain tumor (case 8). (A), Reactive astrocytes at right half are located around a metastatic deposit of adenocarcinoma (HE). (B), a mitochondrial type of 8-oxoguanine DNA glycosylase (hOGG1–2a) is expressed in the reactive astrocytes; (C), while oxidized purine-nucleoside triphosphatase (hMTH1) is expressed by the carcinoma cells but not by the reactive astrocytes. (A), bar = 67 μm; (B), 167 μm; and (C), 100 μm.

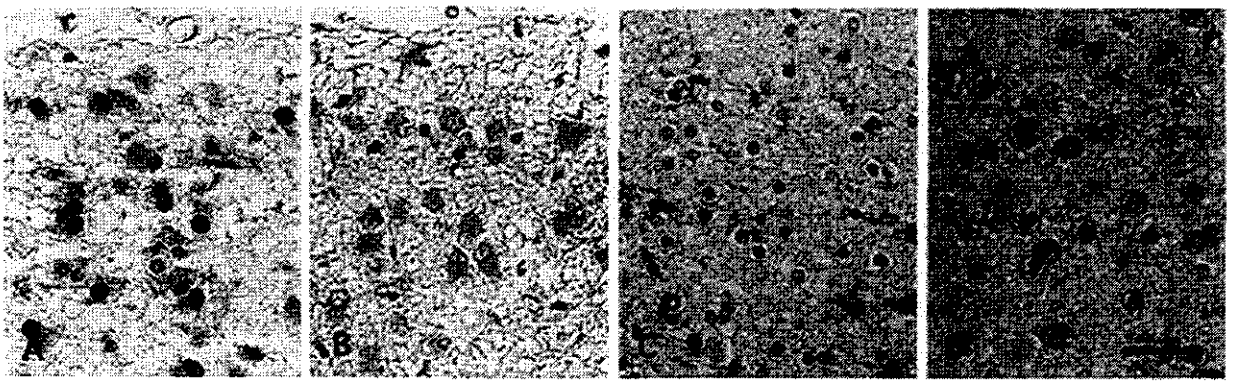

Fig. 3 Immunohistochemistry of cerebral infarction (case 10). Both (A), a mitochondrial type of 8-oxoguanine DNA glycosylase (hOGG1–2a) and (B), oxidized purine-nucleoside triphosphatase (hMTH1) are expressed in cytoplasm of reactive astrocytes around the brain infarct. Nuclear staining for hOGG1–2a is also noted in the astrocytes. Oligodendrocytes around the brain infarct are immunopositive for both hOGG1–2a (C) and hMTH1 (D). (A-D), bar = 33 μm.

immunoreactivities for both repair enzymes were demonstrated in oligodendrocytes. Regarding hOGG1–2a, immunoreactivity of reactive astrocytes was stronger than that of oligodendrocytes. Clinical duration, which means a period from the onset of disease to death, is also documented in Table 1. Taken together with clinical duration and the immunoreactivity, oligodendrocytes tend to be more strongly immunoreactive to the both repair enzymes in cases of acute or subacute stage.

Cell culture under oxidative stress

The results of immunocytochemistry of cultured cells were demonstrated in Fig. 4. We used human glioma cells

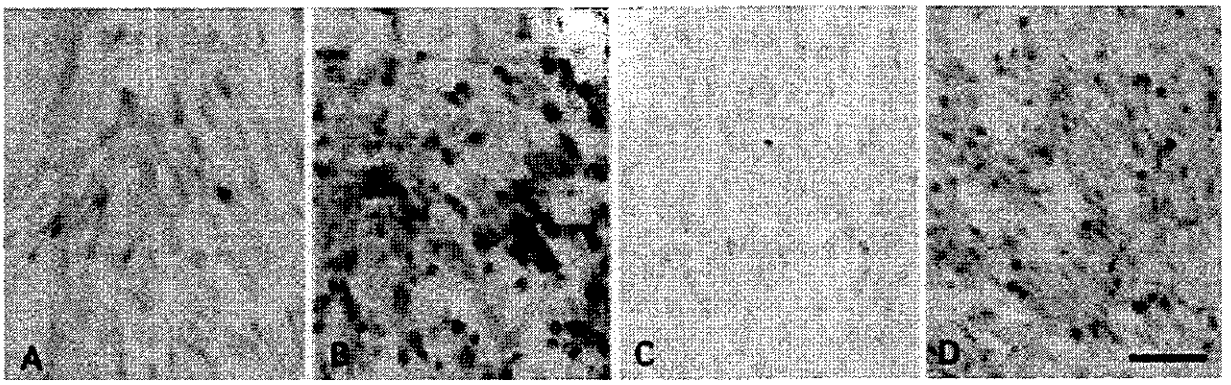

Fig. 4 Immunocytochemistry of cultured glioma cells (KNS81) for (A,B), a mitochondrial type of 8-oxoguanine DNA glycosylase (hOGG1–2a) and (C,D), oxidized purine-nucleoside triphosphatase (hMTH1). (A,C), untreated cells; (B,D), the glioma cells exposed to 10 mmol/L H_2O_2. hOGG1–2a is expressed in both control cells and cells under oxidative stress. hMTH1 is not detected in control cells while accumulated in cells under oxidative stress. (A-D), bar = 33 μm.

(KNS81) to investigate the expression of hMTH1 and hOGG1–2a in glial cells. Because the cells exposed to 20 mmol/L H_2O_2 were almost destroyed, we evaluated cells exposed to 10 mmol/L H_2O_2 as cells under oxidative stress. The hOGG1–2a was expressed in both control cells and cells under oxidative stress, and more intensive immunoreactivity was found in cells under oxidative stress than control cells. Although not expressed in control cells, hMTH1 was induced in cells by adding 10 mmol/L H_2O_2.

DISCUSSION

We previously reported hOGG1–2a expression in reactive astrocytes of Alzheimer's disease brains,[21] and hMTH1 expression in oligodendrocytes and reactive astrocytes.[19] In the present study, we further investigated these phenomena and showed the presence of the protective mechanism to oxidative DNA damage in reactive astrocytes and oligodendrocytes.

In human autopsied brain materials, immunoreactivities to hOGG1–2a were stronger than those to hMTH1 in reactive astrocytes. Indicating the chronic stage of Alzheimer's disease, hOGG1–2a is more strongly expressed than hMTH1 in reactive astrocytes. By adding H_2O_2 to the cultured cells, rapid induction of hMTH1 was observed. However, the immunoreactivity to hOGG1–2a was mildly increased. While acute induction of hMTH1 was observed, hOGG1–2a was constitutively expressed in the untreated cells. These results indicate that hMTH1 is an inducible enzyme under oxidative stress, and hOGG1–2a is rather constitutively expressed and also up-regulated in the chronic stage of disease.

In previous studies, hOGG1–2a was reported to be a mitochondrial type of 8-oxoguanine DNA glycosylase,[15] however, immunoreactivities to hOGG1–2a were recognized not only in the cytoplasm but also in the nuclei of reactive astrocytes. Kikuchi *et al.* described that small aggregates of hMTH1 in the nuclei of the anterior horn cells were present in several ALS cases previously.[26] Although these phenomena might be explained by nuclear accumulation of repair enzymes by its overproduction or oxidative stress in the nucleus itself, its real etiology is unknown. Further studies are necessary to resolve these mechanisms.

Oligodendrocytes are also liable to oxidative stress and are reported as follows. Oligodendroglial precursor cells are exquisitively sensitive to reactive oxygen species,[7] and oligodendroglial maturation is associated with decreased susceptibility to oxidative stress.[6] Oligodendrocytes were vulnerable to free radical damage, which leads to delayed cell death.[8,9] Furthermore, oligodendrocytes are more sensitive to oxidative and nitrative stress *in vitro* than are astrocytes and microglia.[10]

Similar immunoreactivities to both repair enzymes were demonstrated in oligodendrocytes in cases of metastatic tumors. In cases of brain infarcts, oligodendrocytes tend to be more strongly immunoreactive to both repair enzymes in cases of shorter clinical duration, especially acute or subacute cases. Regarding hOGG1–2a in metastatic brain tumors, immunoreactivities of reactive astrocytes are stronger than those of oligodendrocytes. These results suggest the existence of different up-regulating systems in the repair enzymes of different pathological components.

In conclusion, defense mechanisms of glial cells by hMTH1 and hOGG1–2a to oxidative DNA damage are regulated in different manners.

ACKNOWLEDGMENTS

We thank for Ms K. Hatanaka for her excellent technical assistance.

REFERENCES

1. Manganaro F, Chopra VS, Mydlarski MB, Bernatchez G, Schipper HM. Redox perturbations in cysteamine-stressed astroglia: implications for inclusion formation and gliosis in the aging brain. *Free Radic Biol Med* 1995; **19**: 823–835.
2. Papadopoulos MC, Koumenis IL, Yuan TY, Giffard RG. Increasing vulnerability of astrocytes to oxidative injury with age despite constant antioxidant defenses. *Neuroscience* 1998; **82**: 915–925.
3. Wilson JX. Antioxidant defense of the brain: a role for astrocytes. *Can J Physiol Pharmacol* 1997; **75**: 1149–1163.
4. Dalton T, Pazdernik TL, Wagner J, Samson F, Andrews GK. Temporalspatial patterns of expression of metallothionein-I and -III and other stress related genes in rat brain after kainic acid-induced seizures. *Neurochem Int* 1995; **27**: 59–71.
5. Sagara J, Makino N, Bannai S. Glutathione efflux from cultured astrocytes. *J Neurochem* 1996; **66**: 1876–1881.
6. Back SA, Gan X, Li Y, Rosenberg PA, Volpe JJ. Maturation-dependent vulnerability of oligodendrocytes to oxidative stress-induced death caused by glutathione depletion. *J Neurosci* 1998; **18**: 6241–6253.
7. Husain J, Juurlink BH. Oligodendroglial precursor cell susceptibility to hypoxia is related to poor ability to cope with reactive oxygen species. *Brain Res* 1995; **698**: 86–94.
8. Laszkiewicz I, Mouzannar R, Wiggins RC, Konat GW. Delayed oligodendrocyte degeneration induced by brief exposure to hydrogen peroxide. *J Neurosci Res* 1999; **55**: 303–310.
9. Richter-Landsberg C, Vollgraf U. Mode of cell injury and death after hydrogen peroxide exposure in cultured oligodendroglia cells. *Exp Cell Res* 1998; **244**: 218–229.
10. Smith KJ, Kapoor R, Felts PA. Demyelination: the role of reactive oxygen and nitrogen species. *Brain Pathol* 1999; **9**: 69–92.
11. Thorburne SK, Juurlink BH. Low glutathione and high iron govern the susceptibility of oligodendroglial precursors to oxidative stress. *J Neurochem* 1996; **67**: 1014–1022.
12. Maki H, Sekiguchi M. MutT protein specifically hydrolyses a potent mutagenic substrate for DNA synthesis. *Nature* 1992; **355**: 273–275.
13. Michaels ML, Cruz C, Grollman AP, Miller JH. Evidence that MutY and MutM combine to prevent mutations by an oxidatively damaged form of guanine in DNA. *Proc Natl Acad Sci USA* 1992; **89**: 7022–7025.
14. Tchou J, Kasai H, Shibutani S *et al.* 8-oxo-guanine (8-hydroxyguanine) DNA glycosylase and its substrate specificity. *Proc Natl Acad Sci USA* 1991; **88**: 4690–4694.
15. Nishioka K, Ohtsubo T, Oda H *et al.* Expression and differential intracellular localization of two major forms of human 8-oxoguanine DNA glycosylase encoded by alternatively spliced OGG1 mRNAs. *Mol Biol Cell* 1999; **10**: 1637–1652.
16. Fujikawa K, Kamiya H, Yakushiji H, Fujii Y, Nakabeppu Y, Kasai H. The oxidized forms of dATP are substrates for the human MutT homologue, the hMTH1 protein. *J Biol Chem* 1999; **274**: 18201–18205.
17. Sakumi K, Furuichi M, Tsuzuki T *et al.* Cloning and expression of cDNA for human enzyme that hydrolyzes 8-oxo-dGTP, a mutagenic substrate for DNA synthesis. *J Biol Chem* 1993; **268**: 23524–23530.
18. Sekiguchi M. MutT-related error avoidance mechanism for DNA synthesis. *Genes Cells* 1996; **1**: 139–145.
19. Furuta A, Iida T, Nakabeppu Y, Iwaki T. Expression of hMTH1 in the hippocampi of control and Alzheimer's disease. *Neuroreport* 2001; **12**: 2895–2899.
20. Iida T, Furuta A, Kawashima M, Nishida J, Nakabeppu Y, Iwaki T. Accumulation of 8-oxo-2′-deoxyguanosine and increased expression of hMTH1 protein in brain tumors. *Neuro-Oncol* 2001; **3**: 73–81.
21. Iida T, Furuta A, Nishioka K, Nakabeppu Y, Iwaki T. Expression of 8-oxoguanine DNA glycosylase is reduced and associated with neurofibrillary tangles in Alzheimer's disease brain. *Acta Neuropathol (Berl)* 2002; **103**: 20–25.
22. Furuta A, Price DL, Pardo CA *et al.* Localization of superoxide dismutases in Alzheimer's disease and Down's syndrome neocortex and hippocampus. *Am J Pathol* 1995; **146**: 357–367.
23. Kakuma T, Nishida J, Tsuzuki T, Sekiguchi M. Mouse MTH1 protein with 8-oxo-7,8-dihydro-2′-deoxyguanosine 5′-triphosphatase activity that prevents transversion mutation. cDNA cloning and tissue distribution. *J Biol Chem* 1995; **270**: 25942–25948.
24. Kang D, Nishida J, Iyama A *et al.* Intracellular localization of 8-oxo-dGTPase in human cells, with special reference to the role of the enzyme in mitochondria. *J Biol Chem* 1995; **270**: 14659–14665.
25. Takeshita I, Takaki T, Nakamura T, Maeyama R, Fukui M, Kitamura K. Established cell lines derived from human gliomas. *Human Cell* 1990; **3**: 255–256.
26. Kikuchi H, Furuta A, Nishioka K, Suzuki SO, Nakabeppu Y, Iwaki T. Impairment of mitochondrial DNA repair enzymes against accumulation of 8-oxo-guanine in the spinal motor neurons of amyotrophic lateral sclerosis. *Acta Neuropathol (Berl)* 2002; **103**: 408–414.

doi:10.1016/j.jmb.2003.12.060 J. Mol. Biol. (2004) 336, 843–850

JMB

Available online at www.sciencedirect.com

SCIENCE DIRECT®

ELSEVIER

Probing the Substrate Recognition Mechanism of the Human MTH1 Protein by Nucleotide Analogs

Hiroyuki Kamiya[1]*, Hiroyuki Yakushiji[2], Laurence Dugué[3] Mitsuhide Tanimoto[1], Sylvie Pochet[3], Yusaku Nakabeppu[2,4] and Hideyoshi Harashima[1]

[1]*Graduate School of Pharmaceutical Sciences Hokkaido University, Kita-12 Nishi-6, Kita-ku, Sapporo 060-0812, Japan*

[2]*Medical Institute of Bioregulation, Kyushu University, 3-1-1 Maidashi Higashi-ku, Fukuoka 812-8582 Japan*

[3]*Unité de Chimie Organique Institut Pasteur, 28, rue Dr Roux, 75724 Paris cedex 15 France*

[4]*CREST, Japan Science and Technology, Japan*

**Corresponding author*

To examine the substrate recognition mechanism of the human MTH1 protein, which hydrolyzes 2-hydroxy-dATP, 8-hydroxy-dATP, and 8-hydroxy-dGTP, ten nucleotide analogs (8-bromo-dATP, 8-bromo-dGTP, deoxy*iso*inosine triphosphate, 8-hydroxy-dITP, 2-aminopurine-deoxyriboside triphosphate, 2-amino-dATP, deoxyxanthosine triphosphate, deoxyoxanosine triphosphate, dITP, and dUTP) were incubated with the MTH1 protein. Of these, the former five nucleotides were hydrolyzed with various efficiencies. The fact that the *syn*-oriented brominated nucleotides were hydrolyzed suggests that the MTH1 protein binds to deoxynucleotides adopting the *syn*-conformation. However, 8-hydroxy-dITP, which lacks the 2-amino group of 8-hydroxy-dGTP, was degraded with tenfold less efficiency as compared with 8-hydroxy-dGTP. In addition, deoxy*iso*inosine triphosphate, lacking the 6-amino group of 2-hydroxy-dATP, was hydrolyzed as efficiently as 8-hydroxy-dGTP, but less efficiently than 2-hydroxy-dATP. These results clarify the effects of the *anti*/*syn* conformation and the functional groups on the 2 and 6 positions of the purine ring on the recognition by the human MTH1 protein.

Keywords: MTH1; substrate recognition; nucleotide analogs; damaged nucleotide; pyrophosphatase

Introduction

Recent studies have suggested the relationship between the formation of reactive oxygen species (ROS), and various biological processes, including mutagenesis, carcinogenesis, neurodegeneration, and aging.[1–3] ROS modify DNA to form oxidative DNA lesions, which potentially alter the genetic information through their mispairing properties.[4] ROS also modify DNA precursors to form oxidatively damaged nucleotides, which are incorporated into DNA by DNA polymerase(s).[4] These two pathways contribute almost equally to the formation of 8-hydroxyguanine in DNA.[5] In addition, we have shown that the oxidized DNA precursors, 2-OH-dATP, 8-OH-dGTP, 5-hydroxy-2′-deoxycytidine 5′-triphosphate, and 5-formyl-2′-deoxyuridine 5′-triphosphate, induced chromosomal gene mutations *in vivo*.[6,7] Moreover, the presence of the MutT and MTH1 proteins, which hydrolyze 8-OH-dGTP in the nucleotide pools of *Escherichia coli* and mammalian cells, respectively, indicates that the prevention of 8-OH-dGTP incorporation into DNA is important in organisms.[8,9] Deficiency in this hydrolyzing activity resulted in enhanced mutagenesis and tumor formation in *E. coli* and mice, respectively.[10,11] Thus, these nucleotide pool

Abbreviations used: ROS, reactive oxygen species; 2-OH-dATP, 2-hydroxy-2′-deoxyadenosine 5′-triphosphate; 8-OH-dGTP, 8-hydroxy-2′-deoxyguanosine 5′-triphosphate; 8-OH-dATP, 8-hydroxy-2′-deoxyadenosine 5′-tri-phosphate; 8-OH-dA, 8-hydroxy-2′-deoxyadenosine; 2-OH-rATP, 2-hydroxyadenosine 5′-triphosphate; 8-Br-dGTP, 8-bromo-2′-deoxyguanosine 5′-triphosphate; 8-Br-dATP, 8-bromo-2′-deoxyadenosine 5′-triphosphate; dXTP, 2′-deoxyxanthosine 5′-triphosphate; dOTP, 2′-deoxyoxanosine 5′-triphosphate; 8-OH-dITP, 8-hydroxy-2′-deoxyinosine 5′-triphosphate; 8-OH-dI, 8-hydroxy-2′-deoxyinosine; d*iso*ITP, 2′-deoxy*iso*inosine 5′-triphosphate; 2-NH_2-dPuTP, 2-aminopurine-2′-deoxyriboside 5′-triphosphate; 2-NH_2-dATP, 2-amino-2′-deoxyadenosine 5′-triphosphate; hMTH1, human MTH1; HPLC, high-pressure liquid chromatography; NOE, nuclear Overhauser enhancement.

E-mail address of the corresponding author: hirokam@pharm.hokudai.ac.jp

sanitization enzymes and similar proteins appear to prevent the mutations induced by damaged DNA precursors.

Recently, we found that the hMTH1 protein hydrolyzed 2-OH-dATP and 8-OH-dATP, as well as 8-OH-dGTP.[12] In addition, the hMTH1 protein recognizes 2-OH-rATP as a substrate.[13] Thus, the substrate specificity of the hMTH1 protein is of great interest, in addition to its importance in the elimination of mutagenic nucleotides, because the three deoxy-substrates (2-OH-dATP, 8-OH-dATP, and 8-OH-dGTP) seem to lack a common hydrogen acceptor/donor (Figure 1(a)). We suggested that the adoption of the *syn* conformation was one of the important factors in the substrate recognition by the hMTH1 protein.[12] However, the fact that the hMTH1 protein hydrolyzes 8-hydroxy(ribo)adenosine 5′-triphosphate and 8-hydroxy(ribo)guanosine 5′-triphosphate with much less efficiency than 2-OH-rATP[13] suggests that another recognition mode exists.

To address the substrate recognition mechanism of the hMTH1 protein, we prepared ten nucleotide analogs (8-Br-dATP, 8-Br-dGTP, 8-OH-dITP, *diso*-ITP, 2-NH_2-dPuTP, 2-NH_2-dATP, dXTP, dOTP, dITP, and dUTP) and incubated them with the hMTH1 protein. We found that the former five nucleotides were hydrolyzed with various efficiencies. These data help to clarify the substrate recognition mode of the hMTH1 protein.

Results

Nucleotide analogs

The hMTH1 protein hydrolyzes 2-OH-dATP and 8-OH-dATP, as well as 8-OH-dGTP (Figure 1(a)).[12] To address the substrate specificity of the hMTH1 protein, we prepared ten nucleotide analogs and incubated them with the hMTH1 protein. The first group consisted of 8-Br-dATP and 8-Br-dGTP

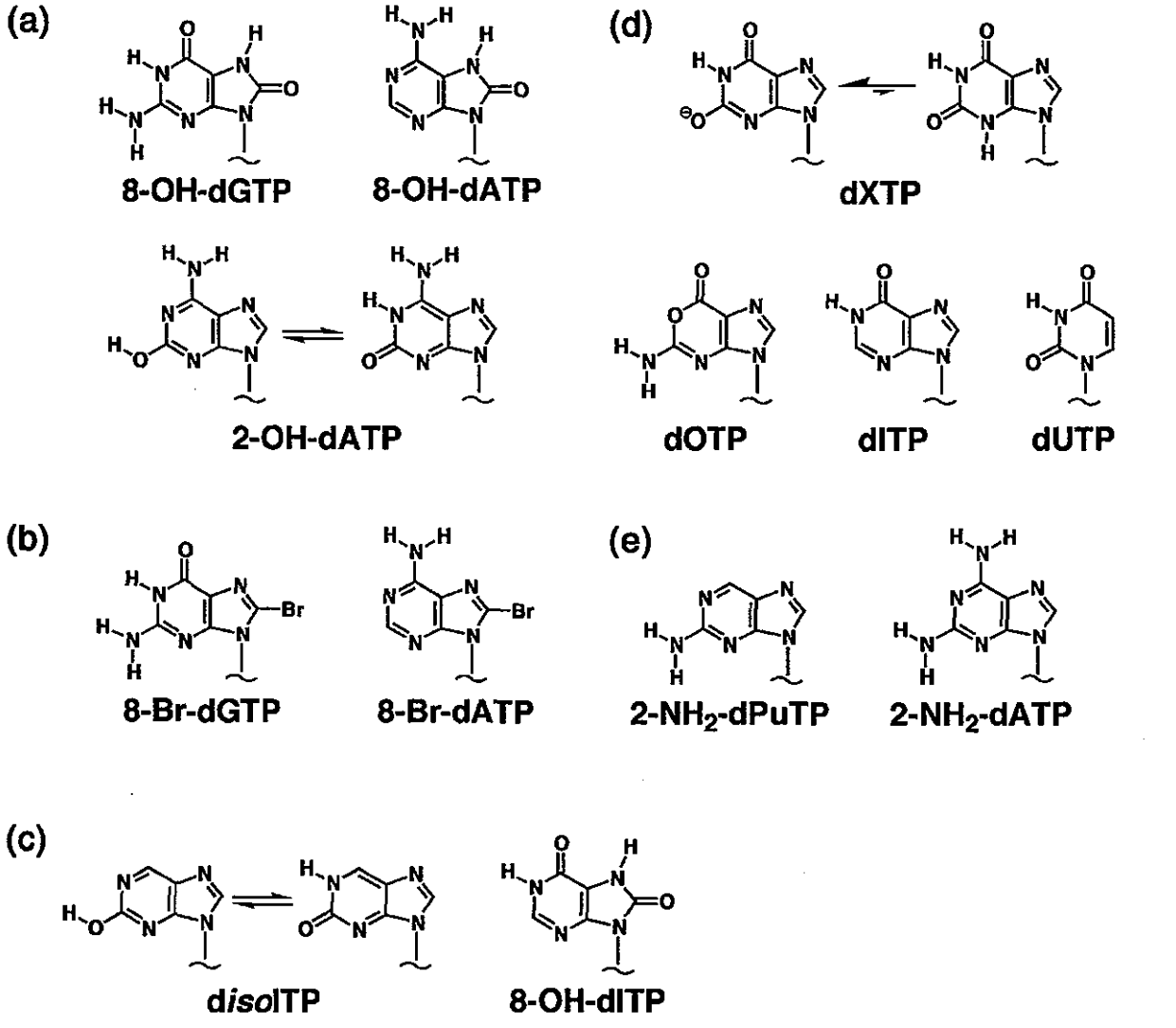

Figure 1. Structures of the base moieties of the nucleotide analogs used in this study. (a) Oxidized nucleotides that are substrates of the hMTH1 protein. (b) The *syn*-oriented nucleotide analogs containing the 8-bromo group. (c) Nucleotide analogs lacking an amino group. (d) Damaged nucleotides formed by nitric oxide. (e) The *anti*-oriented purine nucleotide possessing the 2-amino group.

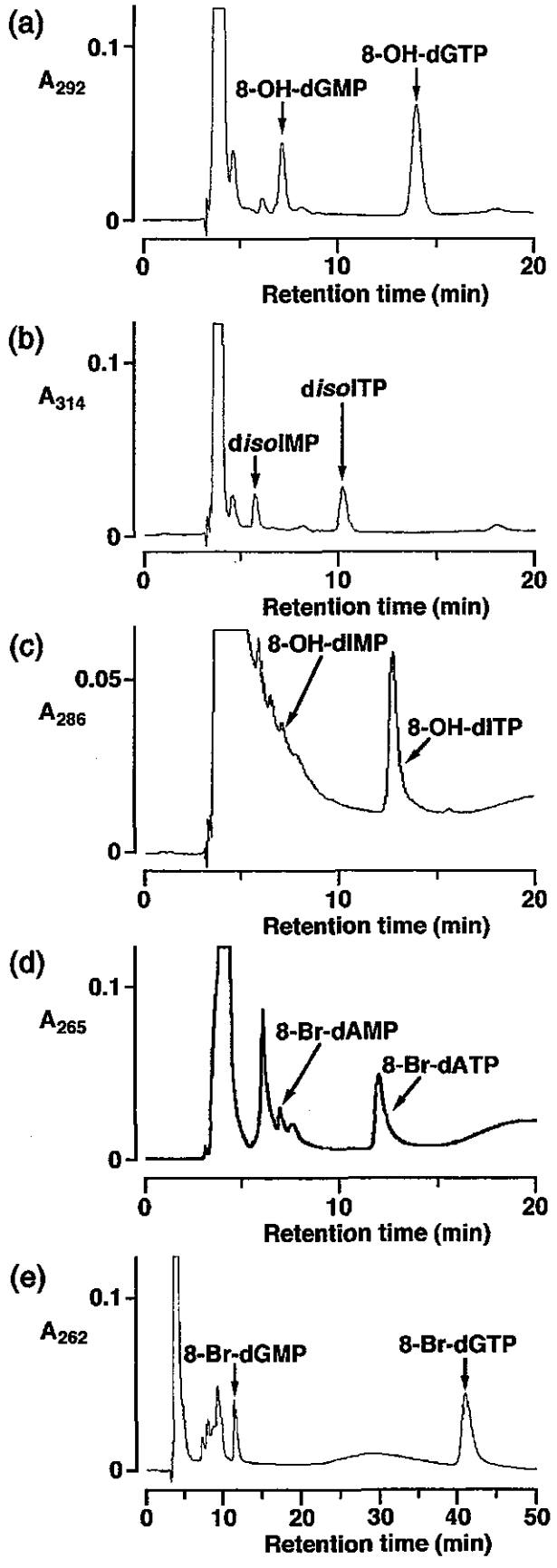

Figure 2. Hydrolysis of nucleotide analogs by the hMTH1 protein, monitored by anion exchange HPLC. Each nucleotide (10 μM) was incubated with 1 nM hMTH1 protein at 30 °C for five minutes. (a) 8-OH-dGTP; (b) *diso*ITP; (c) 8-OH-dITP; (d) 8-Br-dATP; (e) 8-Br-dGTP. (a)–(d) The elution solution was 20% acetonitrile, 75 mM sodium phosphate buffer (pH 7.0). (e) The elution solution was 75 mM sodium phosphate buffer (pH 7.0).

(Figure 1(b)), which are *syn*-oriented analogs of dATP and dGTP, respectively.[14] They differ from 8-OH-dATP and 8-OH-dGTP in their functional groups at the 7 and 8 positions. The second group consisted of *diso*ITP and 8-OH-dITP (Figure 1(c)). The former is an analog of 2-OH-dATP, and lacks the 6-amino group. Likewise, 8-OH-dITP is an analog of 8-OH-dGTP, and lacks the 2-amino group. 8-OH-dITP is also an analog of 8-OH-dATP, and contains the 6-oxo group instead of the 6-amino group of 8-OH-dATP. The third group consisted of 2-NH_2-dPuTP and 2-NH_2-dATP, which contain the 2-amino group (Figure 1(e)).

In addition, we used dXTP, dOTP, dITP, and dUTP, which are damaged nucleotides formed by NO (nitric oxide) (Figure 1(d)), based on the hypothesis that the hMTH1 protein may be involved in the removal of these NO-damaged nucleotides in cells. Moreover, dXTP and dOTP were interesting because they have hydrogen donor and acceptor groups similar to those of the two tautomers of 2-OH-dATP.

Hydrolysis of nucleotide analogs

First, *syn*-oriented 8-Br-dATP and 8-Br-dGTP (10 μM) were incubated with the hMTH1 protein (1 nM). As shown in Figure 2(d) and (e), both nucleotides were hydrolyzed by this enzyme with 0.4 and 0.7-fold efficiencies relative to that of 8-OH-dGTP, respectively (Figure 3). The kinetic parameters obtained indicate that the affinities to these brominated nucleotides were decreased to some degree, as compared with that of 8-OH-dGTP (Figure 4 and Table 1). This reduction in the affinity may be due to the steric hindrance of the bulky bromo group. On the other hand, unmodified dATP is not hydrolyzed and dGTP is a very poor substrate.[12] The fact that the *syn*-oriented purine nucleotides tested were hydrolyzed with efficiencies comparable to that of 8-OH-dGTP (Figure 3) suggests the importance of the *N*-glycosyl bond conformation in the substrate recognition by the hMTH1 protein.

Next, *diso*ITP and 8-OH-dITP were incubated with the hMTH1 protein to examine the importance of the amino groups of 2-OH-dATP and 8-OH-dGTP. We found that *diso*ITP was hydrolyzed as efficiently as 2-OH-dATP by the hMTH1 protein (Figures 2(b) and 3). Thus, the 6-amino group of 2-OH-dATP was not absolutely required for the recognition. However, the loss of the 6-amino group resulted in a threefold increase in the K_m value for *diso*ITP (Table 1). Thus, the 6-amino group of 2-OH-dATP may contribute to the high affinity of this nucleotide for the hMTH1

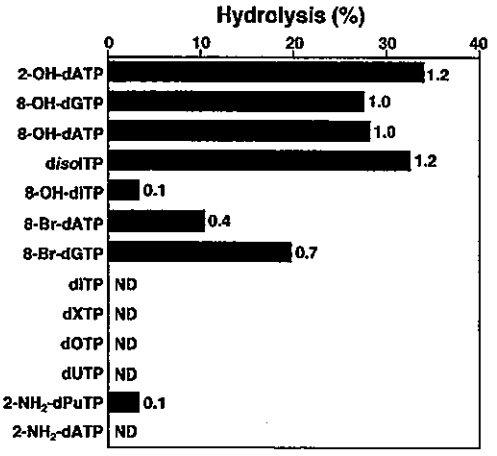

Figure 3. Comparison of the hydrolysis efficiencies of nucleotide analogs by the hMTH1 protein. Each nucleotide (10 μM) was incubated with 1 nM hMTH1 protein at 30 °C for five minutes, and the hydrolysis percentage was measured by HPLC, as described in Materials and Methods. The horizontal axis indicates the hydrolysis percentage for the total substrate added. Relative efficiencies to that of 8-OH-dGTP are shown on the right side of each bar. Experiments were done at least in duplicate and the mean values are represented. ND, not detected.

protein. Although the affinity of *diso*ITP to the hMTH1 protein was lower than that of 2-OH-dATP, due to the loss of the 6-amino group, it was still comparable to that of 8-OH-dGTP. On the other hand, 8-OH-dITP was degraded by the hMTH1 protein with tenfold less efficiency than 8-OH-dGTP (Figures 2(c) and 3). This result suggests that the 2-amino group of 8-OH-dGTP is very important for the recognition of 8-OH-dGTP. 8-OH-dITP is also an analog of 8-OH-dATP, and contains the 6-oxo group instead of the 6-amino group of 8-OH-dATP. From this viewpoint, the 6-amino group of 8-OH-dATP may be involved in the recognition by the hMTH1 protein. However, as shown above, the 6-amino group of 2-OH-dATP was not absolutely required for the recognition. On the basis of the two contrasting results, we speculate that the presence of a hydrogen-donating group at either the 2 or 6 position of a *syn*-oriented purine deoxynucleotide is important for the recognition by the hMTH1 protein.

2-NH_2-dPuTP and 2-NH_2-dATP were then examined, because they have a hydrogen-donating (amino) group at the 2 position. 2-NH_2-dATP, also known as 2,6-diaminopurine-2′-deoxyriboside 5′-triphosphate, has two amino groups at the 2 and 6 positions. When 2-NH_2-dPuTP and 2-NH_2-dATP were incubated with the hMTH1 protein, only 2-NH_2-dPuTP was hydrolyzed, albeit to a lesser degree than 8-OH-dGTP and 2-OH-dATP (Figure 3). The affinity of 2-NH_2-dPuTP was 17-fold less than that of 2-OH-dATP (Table 1). Unmodified dATP containing the 6-amino function is not a substrate of the hMTH1 protein.[12] Thus, the mere presence of a hydrogen-donating group at the

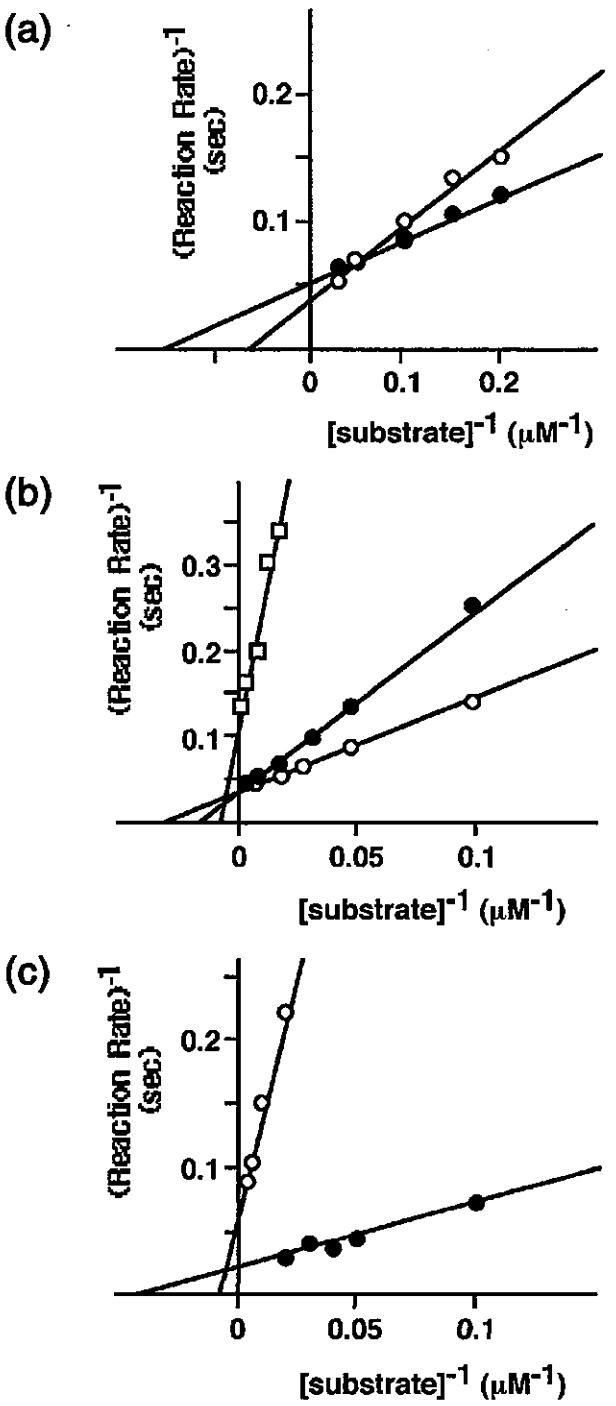

Figure 4. Lineweaver–Burk plots for the hMTH1 activities. The data were obtained from the HPLC assay, as described in Materials and Methods. (a) 8-OH-dGTP (open circles) and 2-OH-dATP (filled circles). (b) 8-Br-dGTP (open circles), 8-Br-dATP (filled circles), and 2-NH_2-dPuTP (open squares). (c) 8-OH-dITP (open circles) and *diso*ITP (filled circles).

2 and 6 positions of a purine deoxynucleotide is not sufficient for recognition by the hMTH1 protein.

Finally, the hypothesis that damaged nucleotides formed by NO, as well as oxidized dATP and dGTP, might be hydrolyzed by the hMTH1 protein

Table 1. Kinetic parameters of nucleotide analogs for the hMTH1 protein

Nucleotide	K_m[a] (μM)	k_{cat}[a] (s^{-1})	k_{cat}/K_m[b] (s^{-1} μM^{-1})
2-OH-dATP	6.8 (6.7, 6.9)	19.2 (19.1, 19.3)	2.82 (1.8)
8-OH-dGTP	17.3 (17.1, 17.5)	27.1 (26.9, 27.3)	1.57 (1.0)
diso ITP	22.5 (22.0, 22.9)	44.8 (43.3, 46.3)	1.99 (1.3)
8-OH-dITP	123.6 (112.4, 134.9)	15.0 (14.4, 15.5)	0.12 (0.1)
8-Br-dATP	63.6 (59.5, 67.8)	28.8 (28.0, 29.7)	0.45 (0.3)
8-Br-dGTP	34.2 (32.4, 36.0)	27.9 (26.1, 29.7)	0.82 (0.5)
2-NH_2-dPuTP	112.4 (93.9, 130.9)	9.6 (9.3, 9.8)	0.09 (0.1)

[a] Experiments were done in duplicate and the mean values are represented. The data obtained in a single experiment are shown in parentheses.
[b] Relative values to 8-OH-dGTP are shown in parentheses.

was examined. dXTP and dOTP were generated from dGTP, and dITP and dUTP are products of dATP and dCTP, respectively (Figure 1(d)). However, none of the four nucleotides was degraded by the hMTH1 protein (Figure 3). Thus, the hMTH1 protein does not act on these four nucleotides formed by nitric oxide.

Discussion

We previously suggested that the *syn* nucleotides could be hydrolyzed by the hMTH1 protein.[12] In this study the two 8-brominated purine nucleotides, 8-Br-dATP and 8-Br-dGTP, were found to be hydrolyzed with 0.4 and 0.7-fold efficiencies, respectively, relative to that of 8-OH-dGTP (Figure 3). On the other hand, dATP was not hydrolyzed by hMTH1, and dGTP was hydrolyzed much less efficiently than 8-OH-dGTP.[12] These brominated nucleotides contain the 8-bromo group instead of the proton of the unmodified compounds (Figure 1(b)). It is difficult to speculate whether the bromo groups are involved in the binding to the hMTH1 protein. In addition, 8-OH-dGTP and 8-OH-dATP have a 7,8-dihydro-8-oxo structure (Figure 1(a)), which differs greatly from the 8-bromo groups of 8-Br-dATP and 8-Br-dGTP. Since they adopt the *syn* conformation,[14] a probable explanation for the recognition is the conformation of the *N*-glycosyl bond. This scenario agrees well with our previous speculation. The fact that 8-OH-dATP and *diso* ITP were hydrolyzed efficiently by hMTH1[12] (Figure 3) suggests that both the 2 and 6-amino groups are dispensable. However, 8-OH-dITP, which also adopts the *syn* conformation,[13] was not a good substrate for the hMTH1 protein (Figures 2(c) and 3). Taken together, these results suggest that a *syn*-oriented purine nucleotide with a hydrogen-donating group at either the 2 or 6-position is recognized. The affinity for *diso* ITP was decreased by the loss of the 6-amino group of 2-OH-dATP (Table 1), but was still comparable with that for 8-OH-dGTP. Thus, favorable interaction(s) may be present between *diso* ITP and the hMTH1 protein.

In the case of 2-hydroxyadenine, the two tautomers, the 2-hydroxy (enol) and 1,2-dihydro-2-oxo (keto) isomers, are present.[15,16] Likewise, the base moiety of *diso* ITP exists as a mixture of the corresponding tautomers.[17] It was reported that the equilibrium between the keto and enol forms of 2-hydroxyadenine shifts in the direction of the enol form with a decrease in the solvent polarity.[15,16] Proteins are more hydrophobic than water, and the equilibrium of 2-OH-dATP might shift to the enol form near/on the hMTH1 protein. By analogy, the population of the enol tautomer of *diso* ITP might increase in a similar situation. These enol tautomers have a hydrogen-donating group at the 2 position (Figure 1(a) and (c)). The hMTH1 protein may bind with these tautomers. This hypothesis could be the reason for the highest affinity of 2-OH-dATP. The enol tautomer of this nucleotide has two hydrogen-donating groups at the 2 and 6 positions. The two favorable interactions between the nucleotide and the amino acid residue(s) may optimize the affinity of 2-OH-dATP. Moreover, *diso* ITP showed an affinity similar to that for 8-OH-dGTP. 8-OH-dGTP has the 2-amino group, and this hydrogen-donating group is located in the same position as the 2-hydroxy group in the enol form of *diso* ITP (Figure 1(a) and (c)). The presence of a hydrogen donor (2-amino or 2-hydroxy group) could explain the similar affinities of *diso* ITP and 8-OH-dGTP. However, 2-NH_2-dATP and 2-NH_2-dPuTP were not good substrates (Figure 3), suggesting the importance of the *N*-glycosyl bond conformation.

Alternatively, the keto tautomers of 2-OH-dATP and *diso* ITP might bind to the hMTH1 protein. In this case, the 1-imino proton or the 2-oxo group of the keto tautomers might be involved in the binding. Since 8-OH-dGTP has the 1-imino proton and the 2-amino group (Figure 1(a)), this 1-imino proton would participate in the binding to the hMTH1 protein. However, this speculation could not explain why 8-OH-dITP was hydrolyzed poorly by the hMTH1 protein: 8-OH-dITP also has the 1-imino proton (Figure 1(c)).

Recently, one of the authors (Y.N.) and his colleagues found that the Trp117 → Ala mutant of the hMTH1 protein lacked the 2-OH-dATPase and 8-OH-dGTPase activities, while the Trp117 → Tyr mutant lost the 8-OH-dGTPase activity, but retained the wild-type level of 2-OH-dATPase activity.[18] These results suggest that the binding of

8-OH-dGTP to the hMTH1 protein depends on the $\pi-\pi$ interaction between the Trp residue and the base moiety more than that of 2-OH-dATP. The different stacking interaction between the base moiety and the Trp residue might indicate that the positions of the 8-hydroxyguanine and 2-hydroxyadenine bases in the binding pocket are slightly different. The interaction between the 7-8-oxo structure and the amino acid residue(s), if present, might explain this putative different location. In this situation, the possibility that the keto tautomers of 2-OH-dATP and *diso*ITP bind the hMTH1 protein could not be excluded. The 1-imino group of the keto tautomers of 2-OH-dATP and *diso*ITP, and the 2-amino group of 8-OH-dGTP could be recognized by the same residue. The base moiety of 8-OH-dITP might be located in a similar position to that of 8-OH-dGTP, due to the 7H-8-oxo structure in the binding pocket, and a deficiency in the interaction between the hMTH1 protein and the 2-amino group might result in the weak binding of the nucleotide. Alternatively, the loss of the electron-donating 2-amino group of 8-OH-dGTP might impair the $\pi-\pi$ interaction between the Trp residue and the base moiety of 8-OH-dITP.

When incubated with the hMTH1 protein, 2-NH_2-dATP, dXTP, and dOTP were not hydrolyzed, and 2-NH_2-dPuTP was hydrolyzed only slightly (Figure 3). 2-NH_2-dATP, 2-NH_2-dPuTP, and dOTP possess hydrogen donor (and acceptor) groups similar to those of the enol tautomer of 2-OH-dATP, on the 1 and 2 positions of their purine rings (Figure 1). On the other hand, dXTP contains hydrogen donor (and acceptor) groups similar to those of the keto tautomer of 2-OH-dATP, on the 1 and 2 positions (Figure 1). However, they were not good substrates, indicating that the hydrogen bonding is not the primary factor for the substrate recognition by the hMTH1 protein.

By NOE measurement of the nucleotide analogs and its ribo derivatives, the ratios of the *syn* conformers in ^2H_2O were estimated as follows: 2-OH-dATP (predominantly the 2-oxo tautomer), 41%; *diso*ITP (also predominantly the 2-oxo tautomer), 21%; dXTP, 12%; dITP, 24%; dOTP, 55%; 2-NH_2-dPuTP, 26%; 2-NH_2-dATP, 21% (H.K. *et al.*, unpublished results).[19] In the case of 2-hydroxy-dA (2-OH-dA), the ratio of the *syn* conformer appeared to depend on the surrounding environment. The ratio of the *syn* conformer was 56% in ^2H_2O and increased to 67% in DMSO-d_6 (H.K. *et al.*, unpublished results). Because the enol–keto equilibrium shifts to the direction of the enol form by increasing the hydrophobicity,[15,16] the ratio of the 2-enol tautomer was higher in DMSO than in H_2O (^2H_2O). Probably, the increase in the *syn* conformer was correlated with increase in the 2-enol tautomer. Thus, the enol tautomer of 2-OH-dA seems to adopt the *syn* conformation, and a similar situation may be present in the case of 2-OH-dATP, and possibly in the case of *diso*ITP. The ratio of the *syn* conformer of dOTP, which was not hydrolyzed by the hMTH1 protein, was relatively high. This discrepancy may be related to the fact that the ring oxygen atom of dOTP has an sp^3 hybrid orbital. Since it has been shown by X-ray diffraction that the six-membered lactone ring is planar,[20] the lone pair electrons of the ring oxygen atom exist out of the plane. Thus, the hMTH1 protein may not recognize dOTP.

As shown in Figure 3, dXTP, dOTP, dITP, and dUTP were not hydrolyzed by the hMTH1 protein. Thus, the hMTH1 protein does not act on these four nucleotides formed by NO. In addition, this result suggests that other enzyme(s), but not the hMTH1 protein, may be involved in the elimination of the damaged nucleotides formed by NO. Indeed, the genes for human dITPase[21] and dUTPase[22] have been reported. The human dITPase may hydrolyze dXTP, because it degrades the corresponding ribonucleotide.[21]

In this study, we have shown that the *anti/syn* conformation and the functional groups on the 2 and 6 positions of the purine ring were important factors in the substrate recognition mechanism of the hMTH1 protein. To reveal the actual binding mode, the structural analysis of the complex of a substrate analog and the protein will be very useful. Experiments toward this goal are in progress.

Materials and Methods

Synthesis of 8-hydroxy-dI

8-OH-dA was synthesized from 2′-deoxy-8-methoxyadenosine,[23] following the procedure described for 2′-deoxy-8-methoxyguanosine.[24] Thus, the treatment of 2′-deoxy-8-methoxyadenosine by *thio*phenol, in the presence of triethylamine in dimethylformamide (DMF) at 50 °C, afforded 8-OH-dA in a 71% yield after purification by silica gel chromatography (dichloromethane/methanol). The 8-OH-dA was then subjected to enzymatic deamination, as described for adenosine and 2′-deoxyadenosine. The treatment of 8-OH-dA with adenosine deaminase from calf intestinal mucosa (type II; Sigma) in 20 mM phosphate buffer (pH 7.4) afforded 8-OH-dI in a 76% yield after purification by silica gel chromatography (dichloromethane:methanol). ^1H NMR (DMSO-d_6) δ: 2.01 (m, 1H, H2′), 2.95 (m, 1H, H2″), 3.57 (m, 1H, H5′), 3.62 (m, 1H, H5″), 3.77 (m, 1H, H4′), 4.36 (m, 1H, H3′), 4.81 (s broad, 1H, 5′-OH), 5.19 (d, 1H, 3′-OH, $J = 4.2$ Hz), 6.13 (t, 1H, H1′, $J = 6.9$ Hz), 8.00 (s, 1H, H2), 11.20 (s broad, 2H, NH). ^{13}C NMR (DMSO-d_6) δ: 34.04 (C2′), 62.71 (C5′), 75.78 (C3′), 82.27 (C1′), 85.25 (C4′), 109.45, 114.78, 145.68 (C2), 151.66, 152.3.

Synthesis of 8-OH-dITP

The 5′-triphosphate derivative was obtained by the condensation of tri-*n*-butylammonium pyrophosphate and the 5′-monophosphate nucleoside, activated as the phosphomorpholidate intermediate according to Moffat.[25] The 8-OH-dITP was isolated after purification by DEAE-cellulose column chromatography in a 40% yield from the free nucleoside, 8-OH-dI. ^1H NMR (^2H_2O) δ: 2.29 (m, 1H, H2′), 3.17 (m, 1H, H2″), 4.05-4.25 (m, 3H, H4′, H5′ and H5″), 4.75 (m, 1H, H3′), 6.27 (t, 1H,

H1′, $J = 7.1$ Hz), 8.09 (s, 1H, H2). ^{31}P NMR (^2H_2O) δ: −21.23 (t, $J = 19.4$ Hz), −9.81 (d), −7.53 (d). ES-MS, negative mode, sample taken in acetonitrile and water, pH 9. Calculated for $C_{10}H_{15}N_4O_{14}P_3$, 508; found, 529 (M-2H + Na), 507 (M − H).

Other nucleotides

The *diso* ITP was synthesized as described.[26] The dXTP and dOTP were prepared by the reported procedures.[27] The 8-Br-dATP and 8-Br-dGTP were synthesized from dATP and dGTP, respectively, by the established methods.[28] The purified dXTP, dOTP, 8-Br-dATP, and 8-Br-dGTP were dephosphorylated with bacterial alkaline phosphatase. The chromatographic behaviors of their dephosphorylated samples and those of the synthetic, authentic samples (kindly provided by Drs Hideo Inoue, Keisuke Makino, and Maki Yamada) were then compared by reverse-phase HPLC, and were found to be identical. The oxidized deoxyribonucleotides, 8-OH-dGTP, 2-OH-dATP, and 8-OH-dATP, were prepared as described.[12,29,30] The dITP and dUTP were purchased from Amersham Bioscience. The 2-NH_2-dPuTP and 2-NH_2-dATP were obtained from TriLink BioTechnologies (San Diego, CA) and were purified by reverse phase HPLC.[29]

MTH1 assay

The hMTH1 protein was obtained by the *E. coli* overexpression system as described.[31] The hMTH1 activities were assayed in a reaction mixture (100 μl) containing 20 mM Tris–HCl (pH 8.0), 4 mM $MgCl_2$, 40 mM NaCl, 80 μg/ml bovine serum albumin, 8 mM dithiothreitol, 10% (v/v) glycerol, and the nucleotide substrates. Following a preincubation at 30 °C for five minutes, the mixtures were incubated at 30 °C with the hMTH1 protein (final concentration, 1 nM). Reactions were terminated by the addition of 100 μl of ice-cold 5 mM EDTA. All samples were injected into a TSK-gel DEAE-2SW column (Tosoh, Tokyo, Japan), with isocratic elution by 75 mM sodium phosphate buffer (pH 7.0) with or without 20% (v/v) acetonitrile, at a flow rate of 1 ml/minute. The amounts of the nucleoside triphosphates and their hydrolyzed products were quantified by measuring the area of UV absorbance. Lineweaver–Burk plots were drawn from the initial velocity of deoxyribonucleoside triphosphatase for the hMTH1 protein. The K_m and k_{cat} values were derived from the intercepts of regression lines.

Acknowledgements

We thank Drs Hideo Inoue, Keisuke Makino and Maki Yamada for providing authentic nucleosides. We also thank Drs John-Stephen Taylor and Noriaki Minakawa for discussions. This work was supported, in part, by Grants-in-Aid from the Ministry of Education, Culture, Sports, Science and Technology of Japan, and from the Kato Memorial Bioscience Foundation.

References

1. Ames, B. N. (1983). Dietary carcinogens and anticarcinogens. *Science*, **221**, 1256–1264.
2. Harman, D. (1981). The aging process. *Proc. Natl Acad. Sci. USA*, **78**, 7124–7128.
3. Ames, B. N., Shigenaga, M. K. & Hagen, T. M. (1993). Oxidants, antioxidants, and the degenerative diseases of aging. *Proc. Natl Acad. Sci. USA*, **90**, 7915–7922.
4. Kamiya, H. (2003). Mutagenic potentials of damaged nucleic acids produced by reactive oxygen/nitrogen species: approaches using synthetic oligonucleotides and nucleotides. *Nucl. Acids Res.* **31**, 517–531.
5. Tajiri, T., Maki, H. & Sekiguchi, M. (1995). Functional cooperation of MutT, MutM and MutY proteins in preventing mutations caused by spontaneous oxidation of guanine nucleotide in *Escherichia coli*. *Mutat. Res.* **336**, 257–267.
6. Inoue, M., Kamiya, H., Fujikawa, K., Ootsuyama, Y., Murata-Kamiya, N., Osaki, T. *et al.* (1998). Induction of chromosomal gene mutations in *Escherichia coli* by direct incorporation of oxidatively damaged nucleotides. *J. Biol. Chem.* **273**, 11069–11074.
7. Fujikawa, K., Kamiya, H. & Kasai, H. (1998). The mutations induced by oxidatively damaged nucleotides, 5-formyl-dUTP and 5-hydroxy-dCTP, in *Escherichia coli*. *Nucl. Acids Res.* **26**, 4582–4587.
8. Maki, H. & Sekiguchi, M. (1992). MutT protein specifically hydrolyses a potent mutagenic substrate for DNA synthesis. *Nature*, **355**, 273–275.
9. Mo, J. Y., Maki, H. & Sekiguchi, M. (1992). Hydrolytic elimination of a mutagenic nucleotide, 8-oxodGTP, by human 18-kilodalton protein: sanitization of nucleotide pool. *Proc. Natl Acad. Sci. USA*, **89**, 11021–11025.
10. Akiyama, M., Horiuchi, T. & Sekiguchi, M. (1987). Molecular cloning and nucleotide sequence of the mutT mutator of *Escherichia coli* that causes A:T to C:G transversion. *Mol. Gen. Genet.* **206**, 9–16.
11. Tsuzuki, T., Egashira, A., Igarashi, H., Iwakuma, T., Nakatsuru, Y., Tominaga, Y. *et al.* (2001). Spontaneous tumorigenesis in mice defective in the MTH1 gene encoding 8-oxo-dGTPase. *Proc. Natl Acad. Sci. USA*, **98**, 11456–11461.
12. Fujikawa, K., Kamiya, H., Yakushiji, H., Fujii, Y., Nakabeppu, Y. & Kasai, H. (1999). The oxidized forms of dATP are substrates for the human MutT homologue, the hMTH1 protein. *J. Biol. Chem.* **274**, 18201–18205.
13. Fujikawa, K., Kamiya, H., Yakushiji, H., Nakabeppu, Y. & Kasai, H. (2001). Human MTH1 protein is highly specific for the oxidized ribonucleotide, 2-hydroxy-ATP. *Nucl. Acids Res.* **29**, 449–454.
14. Uesugi, S. & Ikehara, M. (1977). Carbon-13 magnetic resonance spectra of 8-substituted purine nucleotides. Characteristic shift for the syn conformation. *J. Am. Chem. Soc.* **99**, 3250–3253.
15. Sepiol, J., Kazimierczuk, Z. & Shugar, D. (1976). Tautomerism of isoguanosine and solvent-induced keto-enol equilibrium. *Z. Naturforsch*, **31C**, 361–370.
16. Seela, J., Wei, C. & Kazimierczuk, Z. (1995). Substituent reactivity and tautomerism of isoguanosine and related nucleosides. *Helv. Chim. Acta*, **78**, 1843–1854.
17. Seela, F. & Chen, Y. (1995). Oligonucleotides containing fluorescent 2′-deoxyisoinosine: solid-phase synthesis and duplex stability. *Nucl. Acids Res.* **23**, 2499–2505.

18. Sakai, Y., Furuichi, M., Takahashi, M., Mishima, M., Iwai, S., Shirakawa, M. & Nakabeppu, Y. (2002). A molecular basis for the selective recognition of 2-hydroxy-dATP and 8-oxo-dGTP by human MTH1. *J. Biol. Chem.* **277**, 8579–8587.
19. Chakrabarti, G., Mejillano, M. R., Park, Y.-H., Vander Velde, D. G. & Himes, R. H. (2000). Nucleoside triphosphate specificity of tubulin. *Biochemistry*, **39**, 10269–10274.
20. Nakamura, H., Yagisawa, N., Shimada, N., Takita, T., Umezawa, H. & Iitaka, Y. (1981). The X-ray structure determination of oxanosine. *J. Antibiot.* **34**, 1219–1221.
21. Lin, S., McLennan, A. G., Ying, K., Wang, Z., Gu, S., Jin, H. *et al.* (2001). Cloning, expression, and characterization of a human inosine triphosphate pyrophosphatase encoded by the ITPA gene. *J. Biol. Chem.* **276**, 18695–18701.
22. Ladner, R. D. & Caradonnam, S. J. (1997). The human dUTPase gene encodes both nuclear and mitochondrial isoforms. Differential expression of the isoforms and characterization of a cDNA encoding the mitochondrial species. *J. Biol. Chem.* **272**, 19072–19080.
23. Eason, R. G., Burkhardt, D. M., Phillips, S. J., Smith, D. P. & David, S. S. (1996). Synthesis and characterization of 8-methoxy-2′-deoxyadenosine-containing oligonucleotides to probe the *syn* glycosidic conformation of 2′-deoxyadenosine within DNA. *Nucl. Acids Res.* **24**, 890–897.
24. Koizume, S., Kamiya, H., Inoue, H. & Ohtsuka, E. (1994). Synthesis and thermodynamic stabilities of damaged DNA involving 8-hydroxyguanine (7,8-dihydro-8-oxoguanine) in a ras gene fragment. *Nucleosides Nucleotides*, **13**, 1517–1534.
25. Moffatt, J. G. (1964). A general synthesis of nucleotide-5′ triphosphates. *Can. J. Chem.* **42**, 599–604.
26. Beaussire, J.-J. & Pochet, S. (1999). Recognition of 2′-deoxyisoinosine triphosphate by the Klenow fragment of DNA polymerase I. *Nucleosides Nucleotides*, **18**, 403–410.
27. Suzuki, T., Yoshida, M., Yamada, M., Ide, H., Kobayashi, M., Kanaori, K. *et al.* (1998). Misincorporation of 2′-deoxyoxanosine 5′-triphosphate by DNA polymerases and its implication for mutagenesis. *Biochemistry*, **37**, 11592–11598.
28. Ikehara, M., Tazawa, I. & Fukui, T. (1969). Studies of nucleosides and nucleotides XXXIX. Synthesis of 8-substituted purine nucleotides by the direct replacement reactions. *Chem. Pharm. Bull.* **17**, 1019–1024.
29. Kamiya, H. & Kasai, H. (1995). Formation of 2-hydroxydeoxyadenosine triphosphate, an oxidatively damaged nucleotide, and its incorporation by DNA polymerases. *J. Biol. Chem.* **270**, 19446–19450.
30. Cheng, K. C., Cahill, D. S., Kasai, H., Nishimura, S. & Loeb, L. A. (1992). 8-Hydroxyguanine, an abundant form of oxidative DNA damage, causes G → T and A → C substitutions. *J. Biol. Chem.* **267**, 166–172.
31. Yakushiji, H., Maraboeuf, F., Takahashi, M., Deng, Z. S., Kawabata, S., Nakabeppu, Y. & Sekiguchi, M. (1997). Biochemical and physicochemical characterization of normal and variant forms of human MTH1 protein with antimutagenic activity. *Mutat. Res.* **384**, 181–194.

Edited by J. Doudna

(Received 20 October 2003; received in revised form 12 December 2003; accepted 12 December 2003)

THE JOURNAL OF BIOLOGICAL CHEMISTRY
Vol. 279, No. 32, Issue of August 6, pp. 33806–33815, 2004
Printed in U.S.A.

Structure of Human MTH1, a Nudix Family Hydrolase That Selectively Degrades Oxidized Purine Nucleoside Triphosphates*

Received for publication, March 3, 2004, and in revised form, April 13, 2004
Published, JBC Papers in Press, May 7, 2004, DOI 10.1074/jbc.M402393200

Masaki Mishima,[a] Yasunari Sakai,[b] Noriyuki Itoh,[a] Hiroyuki Kamiya,[c] Masato Furuichi,[b] Masayuki Takahashi,[d] Yuriko Yamagata,[e] Shigenori Iwai,[f] Yusaku Nakabeppu,[b,g] and Masahiro Shirakawa[h,i,j]

From the [a]Graduate School of Biological Sciences, Nara Institute of Science and Technology, 8916-5 Takayama, Ikoma, Nara 630-0101, Japan, [b]Division of Neurofunctional Genomics, Department of Immunobiology and Neuroscience, Medical Institute of Bioregulation, Kyushu University, and Core Research for Evolutional Science and Technology (CREST), Japan Science and Technology Agency (JST), Fukuoka 812-8582, Japan, [c]Graduate School of Pharmaceutical Sciences, Hokkaido University, Kita-12, Nishi-6, Kita-ku, Sapporo 060-0812, Japan, [d]UMR 216, CNRS and Institut Curie, 91405 Orsay, France, Laboratoire de Biocatalyse Faculte des Sciences et des Techniques, FRE2230, CNRS and Universite de Nantes, 2 Rue Houssiniere, 44322 Nantes Cedex 3 France, [e]Graduate School of Pharmaceutical Sciences, Kumamoto University, Oe-honmachi, Kumamoto 862-0973, Japan, [f]Division of Chemistry, Graduate School of Engineering Science, Osaka University, 1-3 Machikaneyama, Toyonaka, Osaka 560-8531, Japan, [h]Graduate School of Integrated Science of Yokohama City University, Suehiro-cho 1-7-26, Tsurumi, Yokohama 230-0045, and [i]Genomic Sciences Center, RIKEN, 1-7-22 Suehiro, Tsurumi, Yokohama, Kanagawa 230-0045, Japan

Oxygen radicals generated through normal cellular respiration processes can cause mutations in genomic and mitochondrial DNA. Human MTH1 hydrolyzes oxidized purine nucleoside triphosphates, such as 8-oxo-dGTP and 2-hydroxy-dATP, to monophosphates, thereby preventing the misincorporation of these oxidized nucleotides during replication. Here we present the solution structure of MTH1 solved by multidimensional heteronuclear NMR spectroscopy. The protein adopts a fold similar to that of *Escherichia coli* MutT, despite the low sequence similarity between these proteins outside the conserved Nudix motif. The substrate-binding pocket of MTH1, deduced from chemical shift perturbation experiments, is located at essentially the same position as in MutT; however, a pocket-forming helix is largely displaced in MTH1 (~9 Å) such that the shape of the pocket differs between the two proteins. Detailed analysis of the pocket-forming residues enabled us to identify Asn^{33} as one of the key residues in MTH1 for discriminating the oxidized form of purine, and mutation of this residue modifies the substrate specificity. We also show that MTH1 catalyzes hydrolysis of 8-oxo-dGTP through nucleophilic substitution of water at the β-phosphate.

Cellular DNA continually suffers assault from exogenous and endogenous agents that cause a wide variety of DNA modifications. Such modifications are often detrimental to the cell, leading to mutagenesis and carcinogenesis. Numerous enzymes have the important task of maintaining the integrity of DNA. These enzymes are generally well conserved from bacteria to humans.

Oxygen radicals, which are spontaneously generated during normal cellular metabolism or by ionizing radiation or various chemicals, often attack nucleic acids, thereby generating modified bases in DNA (1, 2). Among these modified bases, the most abundant species, 8-oxo-7,8-dihydroguanine (8-oxo-G),[1] can pair with both cytosine and adenine with almost equal efficiency and consequently can induce A:T to C:G and G:C to T:A transversion mutations (3–5).

Organisms are equipped with elaborate mechanisms to counteract the mutagenic effects of 8-oxo-G. In *Escherichia coli*, two glycosylases encoded by the *mutM* and *mutY* genes function to prevent mutation caused by the presence of 8-oxo-G in DNA. MutM protein removes 8-oxo-G paired with cytosine, whereas MutY protein removes adenine paired with 8-oxo-G (6–9). To prevent further mutation through the presence of 8-oxo-dGTP, MutT hydrolyzes 8-oxo-dGTP to its monophosphate form, thereby preventing the oxidized purine from being misincorporated into genomic DNA. The importance of this enzyme has been underscored by the observation that deficiency of the *mutT* gene increases the occurrence of A:T to C:G transversion mutations 1000-fold (10, 11). The mechanism concerning the coordinated action of MutM, MutY, and MutT, which constitute the so-called "GO system," has been well characterized in prokaryotes. Protein factors with enzymatic activities similar to those of MutM, MutY, and MutT have been identified in mammals; however, these enzymes show limited sequence similarity to their prokaryotic counterparts (12, 13).

The mammalian counterpart of MutT, MutT homolog-1 (MTH1), is induced after proliferative activation (14), and is predominantly localized in the cytoplasm and mitochondria (15). Mice lacking the *Mth1* gene exhibit an increase in the

* This work was supported in part by grants-in-aid for scientific research (to M. S.) from the Ministry of Education, Culture, Sports, Science, and Technology of Japan, by 21st Century COE Research from Ministry of Education, Culture, Sports, Science, and Technology of Japan (to M. M.), and by the Japan Science and Technology Agency (to M. M. and M. S.). The costs of publication of this article were defrayed in part by the payment of page charges. This article must therefore be hereby marked "*advertisement*" in accordance with 18 U.S.C. Section 1734 solely to indicate this fact.

The atomic coordinates and structure factors (code 1IRY) have been deposited in the Protein Data Bank, Research Collaboratory for Structural Bioinformatics, Rutgers University, New Brunswick, NJ (http://www.rcsb.org/).

[g] To whom correspondence may be addressed. Tel.: 81-92-642-6800; Fax: 81-92-642-6791; E-mail: yusaku@bioreg.kyushu-u.ac.jp.

[j] To whom correspondence may be addressed. Tel.: 81-45-508-7213; Fax: 81-45-508-7361; E-mail: shirakawa@tsurumi.yokohama-cu.ac.jp.

[1] The abbreviations used are: 8-oxo-G, 8-oxo-7,8-dihydroguanine; NOE, nuclear Overhauser effect; NOESY, NOE spectroscopy; TOCSY, total correlation spectroscopy; HSQC, heteronuclear single quantum correlation spectroscopy; r.m.s.d., root mean square deviations; AMPCPP, α,β-methyleneadenosine triphosphate; ADPRase, ADP-ribose pyrophosphatase; 2-OH-dATP, 2-hydroxy-dATP.

occurrence of spontaneous carcinogenesis in liver and, to a lesser extent, in lung and stomach, suggesting that an accumulation of 8-oxo-dGTP, which is a substrate of MTH1, may trigger malignant transformation *in vivo* (16). The detrimental effect of 8-oxo-dGTP in eukaryotes is also implied from the observation that an increase in the accumulation of 8-oxo-G in DNA, together with an increase in the expression of MTH1, is found not only in human cancer tissue (17, 18) but also in degenerating neurons, as determined by immunohistochemical analyses (19, 20).

MTH1, but not *E. coli* MutT, can hydrolyze *in vitro* nucleotide triphosphates containing oxidized adenine such as 2-hydroxy-dATP (2-OH-dATP), 2-OH-rATP, 8-oxo-dATP, and 8-oxo-rATP, in addition to those containing oxidized guanines such as 8-oxo-dGTP and 8-oxo-rGTP (21, 22). Furthermore, MTH1 exerts higher enzymatic activity for 2-OH-dATP than for 8-oxo-dGTP, with Michaelis constant (K_m) values of 8.3 and 15.2 μM, respectively (21). 2-OH-dATP has been shown to induce G:C to T:A transversion mutations (23). These observations suggest that, in addition to 8-oxo-dGTP, oxidized forms of dATP may cause an increase in the incidence of spontaneous carcinogenesis in *Mth1* knockout mice, and thus may be mutagenic. This assumption is supported by the finding that the expression of a D119A mutant of MTH1, which retains half of the wild-type activity for 8-oxo-GTP but is unable to hydrolyze 2-OH-dATP, can only partially suppress cell dysfunction and delayed cell death in *Mth1*-null mouse embryo fibroblasts, whereas the expression of wild-type MTH1 effectively suppresses these phenotypes (24).

The significance of adenine oxidization is further suggested by the following biochemical observations. First, the treatment of cultured human cells with H_2O_2 induces the accumulation of 2-hydroxyadenine in genomic DNA at one-fifth of the level of 8-oxo-G accumulation (25). Second, another mammalian hydrolase, NUDT5, has been shown recently to hydrolyze 8-oxo-dGDP specifically to the monophosphate form, suggesting that the cooperative action of MTH1 and NUDT5 is necessary for the effective elimination of oxidized nucleotides (26). Growing evidence has highlighted the importance of this elaborate system in countering the accumulation of oxidative damaged DNA.

The catalytic site for the hydrolysis reaction of MTH1 is thought to be located at the "Nudix motif," an array of 23 amino acids ($GX_5EX_7REUXEEXGU$, where U represents a bulky hydrophobic amino acid) that is found in a family of conserved hydrolases (27, 28). Substrates of these so-called "Nudix" family hydrolases include various nucleotide and nucleotide derivatives, such as dATP, diadenosine oligophosphates, NADH, and ADP-ribose (29, 30). Despite their apparently low similarity in chemical structure, these substrates commonly contain two phosphates linked by an ester bond that joins a nucleotide to a mono- or polyphosphate, nucleotide, or ribose. Nudix enzymes catalyze the hydrolytic cleavage of this ester bond. The catalytic activities of the Nudix enzymes are generally low; for example, the k_{cat} of MTH1 is of the order of 10^1. The catalytic mechanisms of the Nudix enzymes MutT and Orf17 have been well characterized (29, 31). These enzymes commonly catalyze hydrolytic cleavage of the Pα–Pβ bond in nucleotide triphosphates. In addition, Mildvan and co-workers (29, 31) have shown that the cleavage reaction is initiated by nucleophilic attack by water on the β-phosphate.

In this study, we have determined the solution structure of human MTH1 by heteronuclear multidimensional NMR. Coupled with biochemical analyses, the structure has enabled us to identify the substrate interaction pocket. Furthermore, by means of an established protocol using ^{18}O-enriched water (31), we have identified the substrate β-phosphate that undergoes nucleophilic attack by a water molecule during the hydrolysis reaction.

EXPERIMENTAL PROCEDURES

Sample Preparation—The protein was expressed in *E. coli* BL21(DE3) transfected with a plasmid encoding human MTH1 (32). To achieve uniform ^{15}N and/or ^{13}C labeling, the bacteria were grown in M9 minimal medium with $^{15}NH_4Cl$ and/or [$^{13}C_6$]glucose as the sole source of nitrogen and/or carbon, respectively. For the TROSY-HNCO experiment, a uniformly $^{15}N/^{13}C$-labeled and fractionally deuterated protein sample was prepared by growing bacteria in M9 medium containing 80% ^2H_2O. The cells were grown at 37 °C, and protein expression was induced by adding isopropyl-1-thio-β-D-galactopyranoside when the absorbance at 660 nm reached 0.45. Cells were harvested 4 h after protein induction and resuspended in 50 mM Tris buffer (pH 7.5) containing 500 mM KCl, 10 mM dithiothreitol, and 1 mM EDTA. The suspension was lysed by sonication and ultracentrifuged, and the resultant supernatant was loaded onto a DEAE-Sepharose column. The flow-through fraction was collected, concentrated by ammonium sulfate saturation, and passed through a phenyl-Sepharose column (Amersham Biosciences). Finally, the protein was purified by passage through a Sephacryl S-100 (Amersham Biosciences) gel filtration column. Protein concentrations were estimated by using the calculated molar absorption coefficient at 280 nm ($\epsilon_{280} = 28 \times 10^3\ M^{-1}\ cm^{-1}$).

Sequence Alignment—The primary sequences of human MTH1 and MutT were manually aligned on the basis of the fitted tertiary structures of human MTH1 and MutT (Protein Data Bank code 1MUT), assuming insertions and gaps. The sequence of mouse MTH1 is highly homologous to that of human MTH1 and contains the same number of amino acids. Thus, no alignment process was needed, and the murine sequence was fitted to the human MTH1 sequence with no insertions and gaps. Manual alignment procedures were performed by the BioEdit program (33).

Monitoring Isotope Shifts—The MTH1-catalyzed hydrolysis of 8-oxo-dGTP and the isotope shift of the reaction products were monitored by ^{31}P NMR, essentially using the procedure of Mildvan and co-workers (31). The reaction mixture, containing 1 mM 8-oxo-dGTP, 0.6 μg/ml MTH1, 50 mM Tris buffer (pH 9.0), 10% ^2H_2O and 0, 24, or 48% $H_2{}^{18}O$, was incubated at 30 °C. After 120 min, the reaction was stopped with excess EDTA. One-dimensional ^{31}P NMR spectra were obtained at 202.45 MHz on a Bruker DMX 500 spectrometer equipped with a broad band 5-mm probe.

Structure Determination—Purified MTH1 was dissolved in 50 mM potassium phosphate buffer (pH 6.9) containing 20 mM KCl, 0.1 mM EDTA, and 1 mM dithiothreitol in either 95% H_2O, 5% ^2H_2O or 99.8% ^2H_2O. The final concentration of the protein was adjusted to 1.7 mM and placed in 5-mm diameter micro-NMR cells (Shigemi, Inc.) for multidimensional NMR spectroscopy.

NMR spectra were acquired at 30 °C on a Bruker DMX500, DRX500, or DRX800 NMR spectrometer. Chemical shifts were referenced to 4,4-dimethyl-4-silapentane 1-sulfonate. All multidimensional NMR spectra were acquired in a phase-sensitive mode employing a States-TPPI or Rance-Kay manner (34). The water flip-back method (35) was employed in several experiments, starting from amide proton magnetization. Lorentz-to-Gauss transformations or shifted sine-bell window functions were applied to the NMR data before zero-filling and Fourier transformation. Mirror image or forward-backward linear prediction was used in indirect time domains. All spectra were processed by the NMRPipe package (36), and analyzed by Pipp (36) and Sparky (37).

Assignments of ^1H, ^{13}C, and ^{15}N were obtained from standard multidimensional NMR methods (38). The isopropyl groups of all leucine and valine residues were assigned in a stereospecific manner from the HSQC spectrum of a 15% ^{13}C-enriched sample (39). Hydrogen bond restraints were derived from correlations through $^{h3}J_{NC'}$ couplings (40, 41), which were observed in TROSY-HNCO experiments. Well dispersed side-chain carboxyl ^{13}C resonances of glutamate and aspartate residues were assigned by an $H(C)CO_2$ experiment (42). Interproton distances were derived from two-dimensional NOESY, ^{15}N NOESY-HSQC, four-dimensional $^{13}C/^{15}N$-edited HMQC-NOESY-HSQC, and four-dimensional $^{13}C/^{13}C$-edited HMQC-NOESY-HSQC (38). NOEs were grouped into three upper distance ranges, 2.8, 3.5, and 5.0 (3.2, 4.2, and 5.0 for NOEs involving NH protons), corresponding to strong, medium, and weak peak intensities. NOE intensities were calibrated by using known distances in regular secondary structure elements, and standard pseudo-atom distance corrections were applied to upper bound constraints involving methyl and methylene protons. Aromatic ring protons were represented as a $(\Sigma r^{-6})^{-1/6}$ sum (43).

Backbone dihedral angles were estimated from vicinal coupling constants ($^3J_{HNHA}$) obtained from HNHA experiments (38). The dihedral ϕ angles used were $-60 \pm 40°$ for $^3J_{HNHA} < 4$ Hz and $-120 \pm 40°$ for $^3J_{HNHA} > 8$ Hz. In addition, dihedral ϕ and ψ angles derived from TALOS (44) were used in a final refinement step. If the deviation predicted by TALOS was less than 20°, the value was set to 20°. The program DYANA version 1.5 (45) was used at the stage of structural constraint collection. Finally, an ensemble of 100 MTH1 structures was calculated with the program CNS version 1.0 (46). The calculated structures were analyzed by PROCHECK-NMR (47) and MOLMOL (48), and the graphics were created by MOLMOL, Ribbons (49), or GRASP (50).

Chemical Shift Perturbation—^1H and ^{15}N amide resonance changes in uniformly ^{15}N-labeled MTH1 were monitored after the addition of an equimolar amount of 8-oxo-dGDP or 2-OH-dADP to 20 mM HEPES buffer (pH 6.9) containing 20 mM KCl, 0.1 mM protein, 1 mM EDTA, 1 mM dithiothreitol, and 5% ^2H_2O. The ^1H-^{15}N HSQC spectra were obtained at 30 °C. Changes in signal intensities and chemical shifts were analyzed by Sparky (37). For each cross-peak, the normalized weighted average shift difference, $\delta_{ave}/\delta_{max}$, was calculated (51, 52). The weighted average shift difference, δ_{ave}, was calculated as $\{(\delta_{1H}^2 + (\delta_{15N})^2)/2\}^{1/2}$, where δ_{1H} and δ_{15N} represent the differences in ppm between the free and perturbed chemical shifts. The δ_{max} value represents the maximum observed weighted average shift difference. Changes in signal intensity were also evaluated by the ratio of the intensity differences caused by perturbation and the reference spectrum $(I_{ref} - I_{per})/I_{ref}$, where I_{ref} and I_{per} represent the signal intensities in the reference and perturbed spectrum, respectively.

RESULTS

Structure Determination of MTH1—Recombinant MTH1 was overexpressed in *E. coli*, isotopically labeled, and purified by chromatography on hydrophobic and gel filtration columns. The elution profile derived from gel filtration chromatography suggests that MTH1 exits as a monomer when purified to homogeneity (data not shown). The ^{15}N-^1H HSQC spectrum of MTH gave a highly dispersed pattern of cross-peaks, suggesting that the whole protein molecule adopts a stable tertiary conformation in solution (data not shown).

NMR resonance assignments were obtained by measuring the double and triple resonance NMR spectra of ^{15}N- and ^{15}N,^{13}C-labeled protein samples. Assignments for all of the main-chain resonances, except for those of Met[1], were obtained from the CBCANH, CBCA(CO)NH, HN(CA)CO, and HNCO spectra. Side-chain assignments were essentially obtained from C(CO)NH, H(CCO)NH, HCCH-TOCSY, and four-dimensional HC(CO)NH spectra. By combining the three-dimensional HCCH-TOCSY spectra with the four-dimensional HC(CO)NH, we obtained far less ambiguous correlations between side-chain ^{13}C and ^1H nuclei, which led to reliable side-chain assignments. Most of the aromatic ^1H resonances were obtained from two-dimensional NOESY and ^{13}C-edited NOESY spectra.

The structure of MTH1 was determined from more than 2100 distance and torsion angle constraints, including those for 46 hydrogen bonds that were directly detected through $^{h3}J_{NC'}$ couplings across the bonds in the TROSY-HNCO spectrum. Of these hydrogen bonds, 32 were identified in regions of regular secondary structure, such as antiparallel and parallel β-sheets and α-helices, and 14 were found in regions with no secondary structure. This direct observation of hydrogen bonds was extremely useful in the initial steps of structure determination, because it enabled us to establish unambiguously the topology of the secondary structure, in particular that of the β-strands. Furthermore, it was also helpful for identifying irregular patterns of hydrogen bonding in the β-sheet regions, which are generally difficult to determine by other NMR techniques, such as measuring the rate of amide proton exchange with solvent or NOE patterns (see below). The backbone of the final 30 structures derived from the NMR data (Fig. 1*A*) shows that the atomic coordinates throughout the protein molecule are well defined except for the N- and C-terminal residues. The root mean square deviations (r.m.s.d.) for the averaged structure of the well defined region were 0.44 Å for the backbone and 0.99 Å for all heavy atoms (residues 5–153). The statistics of the structures are shown in Table I.

Structure of MTH1—MTH1 adopts an $\alpha+\beta$ fold with four long loops consisting of seven β-strands and two α-helices as follows: βA (residues 5–11), βB (17–22), βC (67–74), βD (80–87), βE (102–107), βF (132–139), βG (146–153), αI (44–58), and αII (120–130) (Fig. 1*B* and Fig. 2). The main frame of the fold is a curled mixed β-sheet made up of five strands. Whereas most of the residues on the convex side of the sheet form a continuous solvent-accessible surface, those on the concave side are packed against helix αII, loop 4 (L4) linking αII and βE, and loop 1 (L1) linking αI and βB, all of which form the main body of the protein. In addition, a lobe made up of helix αI and an antiparallel two-stranded β-sheet is attached to the main body at strand βA, which forms the edge of the mixed β-sheet. As a consequence, a deep and narrow pocket is formed between this additional lobe and the main body of the protein; this pocket is surrounded by walls comprising helix αI, loop L1, and the mixed sheet (Fig. 1*B* and Fig. 2).

The hydrogen bonds directly observed through $^{h3}J_{NC'}$ couplings across the bonds reveal the presence of a β-bulge between strands C and D in the core β-sheet. In the TROSY-HNCO spectrum used to detect these $^{h3}J_{NC'}$ couplings, a correlation was observed between the carbonyl group of Val[85] and the amide group of Val[67], whereas the amide group of Gly[68] showed no detectable correlations. These observations indicate that a hydrogen bond is formed between Val[85] and Val[67], establishing a small β-bulge structure with a bend at the main-chain position of Gly[68] (Fig. 1*C*).

The Nudix motif, which is located at residues 37–59, is composed of an amphipathic helix of about three turns (α1) and a preceding loop (L1) that adopts a well defined hairpin-like structure (Fig. 1*B* and Fig. 3). This loop contains a type II β-turn formed by residues 40–43, which is characterized by positive ϕ and ψ angles of Gly[42] ($\phi = 108 \pm 32°$ and $\psi = 43 \pm 13°$), and is stabilized by a hydrogen bond formed between the main-chain amide group of Gln[40] and the side-chain carboxyl group of Glu[43]. Both Glu[43] and Gly[42] are conserved in all members of the Nudix enzyme family, suggesting the importance of this β-turn. Notably, an $^{h3}J_{NC'}$ coupling across this hydrogen bond was detected in the TROSY-HNCO experiment, which unambiguously confirms its presence.

Structural Comparison of MTH1 and MutT—Although the sequence identity between human MTH1 and *E. coli* MutT is as low as 9.3% outside the Nudix motif (residues 37–59 of MTH1), the overall folds of these proteins resemble one another (Fig. 4*A*). In particular, the central part of MTH1, comprising β-strands βA, βD, and βC and the Nudix helix (α1), shows high structural similarity to the corresponding part of MutT. This is reflected by the r.m.s.d. between MTH1 and MutT (PDB code 1MUT) of 1.8 Å over 39 Cα coordinates for residues in these regions (MTH1 residues 4–12, 43–58, 67–72, and 80–87).

The largest difference between the structures of MTH1 and MutT is the presence of a β-hairpin comprising strands βF and βG and their connecting loop in MTH1, which is absent in MutT (Fig. 4*A*). Strand βF is connected to βC through a main-chain hydrogen bond network, resulting in the formation of a continuous five-stranded β-sheet made up of strands βA, βD, βC, βF, and βG. Given that residues from the additional β-hairpin make extensive hydrophobic contacts with those from helix αII, the orientation of this helix and the N-terminal half of loop L1 relative to strands βA, βD, and βC in MTH1 differs from the orientation of the corresponding regions in MutT. The helix is

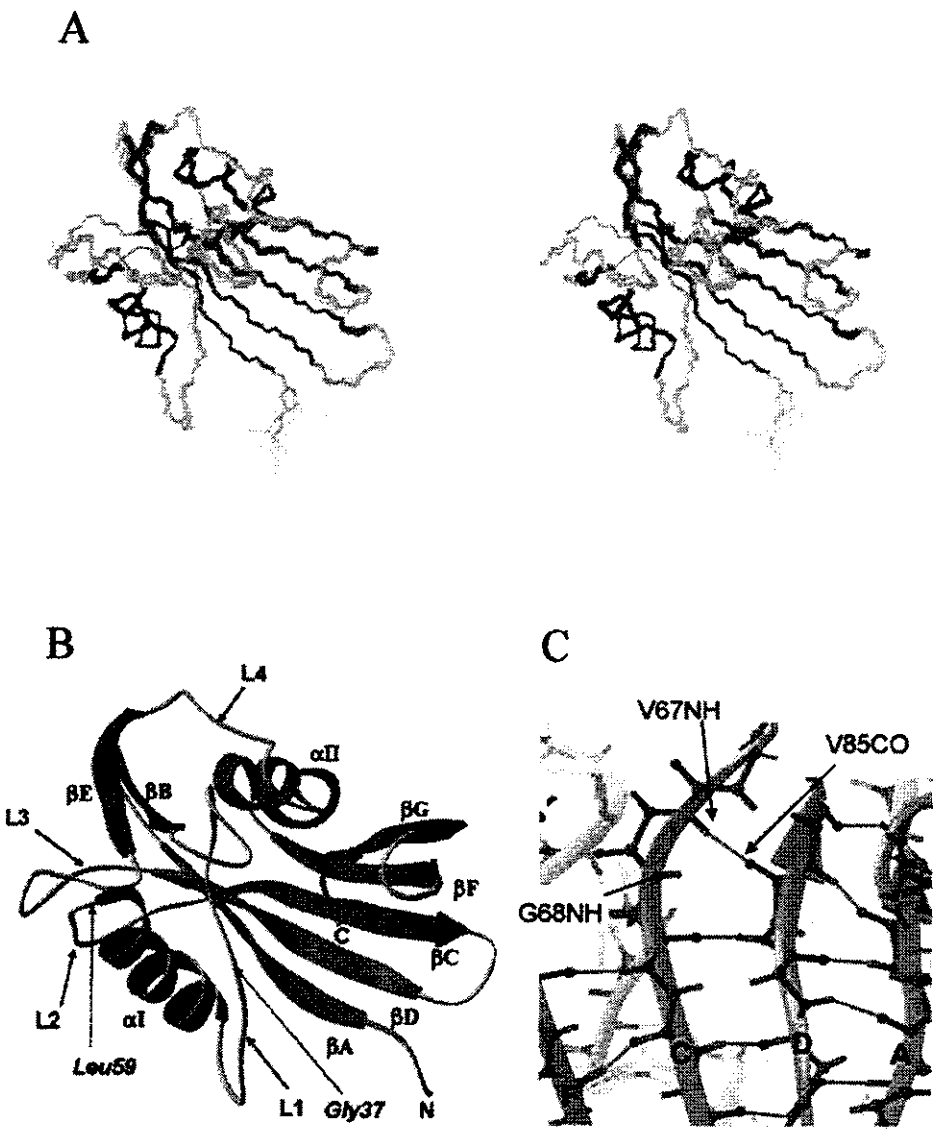

FIG. 1. **Solution structure of MTH1.** *A*, stereo view of the best fit backbone superpositions of the final 30 simulated annealing structures of MTH1. Helices are shown in *red* and strands in *blue*. *B*, schematic ribbon drawing of the representative structure of MTH1. The molecular orientation is nearly the same as in *A*. The start residue Gly^{37} and the end residue Leu^{59} of the Nudix motif are indicated. *C*, the β-bulge at the terminal region of strands βC and βD. Hydrogen bonds (see text) are shown in *pink*. The protein backbone is shown in *ribbon* and *ball-and-stick* representation.

displaced by ~9 Å at the position of the N-terminal residue of helix αII. Previous analyses have shown that deleting the additional strands βF and βG totally abolishes both the 2-OH-dATPase and the 8-oxo-dGTPase activity of MTH1 (53).

Chemical Shift Perturbation Experiments—To identify the substrate-binding site of MTH1, we carried out chemical shift perturbation experiments in which we monitored the cross-peaks of the $^{15}N-^{1}H$ HSQC NMR spectrum by using ^{15}N-labeled MTH1. As substrate analogs, we used 8-oxo-dGDP and 2-OH-dADP, which act as specific inhibitors of the 8-oxo-dGTPase and 2-OH-dATPase activity with K_i values of 0.51 and 0.22 μM, respectively (22). Hydrolysis of these analogs by MTH1 is extremely slow, especially in the absence of magnesium ions (22). We therefore performed the chemical shift perturbation experiments using these oxidized diphosphates in the absence of magnesium so that the substrate-enzyme complex would be stable during the measurements.

Upon mixing MTH1 with 8-oxo-dGDP, large broadening and/or relatively small changes in chemical shift were observed for some signals in the $^{15}N-^{1}H$ HSQC spectrum (Fig. 5*A*). Most of the signals exhibited intermediate exchange on the NMR time scale during the titration. After mixing in an equimolar amount of substrate, the addition of more 8-oxo-dGDP caused no further changes in the HSQC spectra, suggesting that the complex is formed at a 1:1 molar ratio (data not shown). The observed spectral changes were specific to 8-oxo-dGDP because titration with dGTP and dGDP caused no detectable changes in the spectra (data not shown). Most of the residues that showed a large normalized weighted average shift difference ($\delta_{ave}/\delta_{max} > 0.4$) or broadening ($(I_{ref} - I_{per})/I_{ref} > 0.4$ of the original values) upon titration were confined to the inside or rim of a pocket that is formed between the five-stranded mixed sheet, helix αII, and the hairpin loop (Fig. 5*B*), suggesting that this pocket may be the nucleotide-binding site. The inner surface of the pocket is dominated by hydrophobic residues, most signals of which in the $^{15}N-^{1}H$ HSQC spectrum were affected by nucleotide binding (Fig. 5*B* and Fig. 6*A*).

Chemical shift perturbation experiments were also performed in the absence of magnesium ions for the complex formed between 2-OH-dADP and MTH1. As observed for the

TABLE I
Structural statistics for the final 30 NMR structures of hMTH1
All variances are quoted to one S.D.

Total number of distance constraints (NOE)	2135
Long range ($\|i-j\|>4$)	643
Middle range ($\|i-j\|=2$–4)	296
Short range ($\|i-j\|=1$)	555
Intra-residue	549
Hydrogen bond constraints	46 × 2
Dihedral constraints (derived from $^3J_{NH\alpha}$ and TALOS) ϕ, ψ	99, 78
r.m.s.d. from experimental constraints	
Distance (Å)	0.0185 ± 0.0008
Angle (°)	0.530 ± 0.02
r.m.s.d. from idealized covalent geometry	
Bonds (Å)	$0.00227 \pm 8 \times 10^{-5}$
Angles (°)	0.398 ± 0.005
Impropers (°)	0.276 ± 0.006
CNS potential energy (E_{total})	281.7 ± 8.0
PROCHECK Ramachandran plot (5–153)	
Residues in most favored regions	74.3 ± 1.9%
Residues in additional allowed regions	23.0 ± 1.8%
Residues in generously allowed regions	2.61 ± 0.69%
Residues in disallowed regions	0.05 ± 0.20%
r.m.s.d. to mean structure of the calculated 30 structures	
Backbone (5–153)	0.44 Å
All heavy (5–153)	0.99 Å

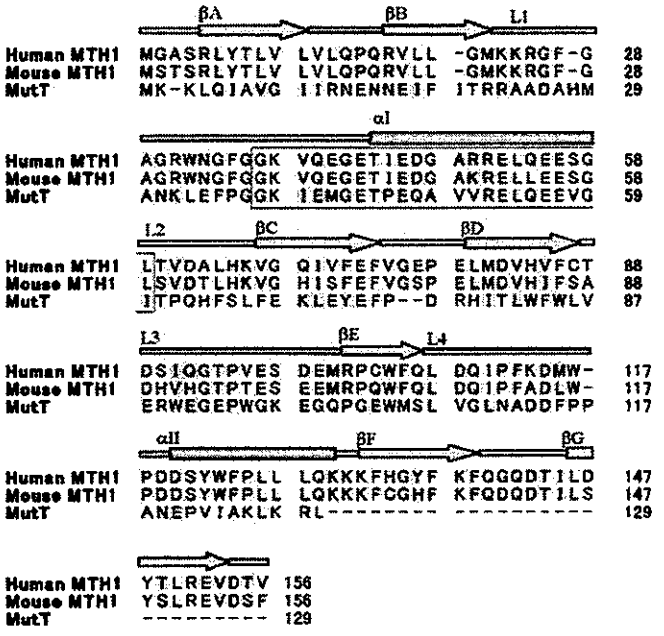

FIG. 2. **Sequence alignment of MTH1 and MutT.** The amino acid sequence alignment of human MTH1, mouse MTH1, and *E. coli* MutT is shown. Conserved residues are shown in *yellow* and homologous residues in *gray*. The secondary structure elements of MTH1 are indicated on *top*. The Nudix motif is *boxed* in *red*.

8-oxo-dGDP titration, residues in the hydrophobic pocket showed a large, normalized, weighted average shift difference ($\delta_{ave}/\delta_{max} > 0.4$) or signal broadening ($(I_{ref} - I_{per})/I_{ref} > 0.4$ of the original values). This result suggests that 2-OH-dADP binds to the same pocket that 8-oxo-dGDP uses (Fig. 5*B* and Fig. 6*A*). More residues around the pocket exhibited signal perturbations after the addition of 2-OH-dADP than after that of 8-oxo-dGDP, suggesting that local conformation changes take place in the proximity of the pocket. It may be possible that the higher affinity of 2-OH-dADP, as compared with 8-oxo-dGDP, may cause larger structural effects on binding. Such a conformational change induced by substrate binding is observed in the pocket of MutT on the binding of 8-oxo-dGMP (54); helix I of MutT moves 4.5 Å toward the Nudix motif such that the pocket becomes narrower.

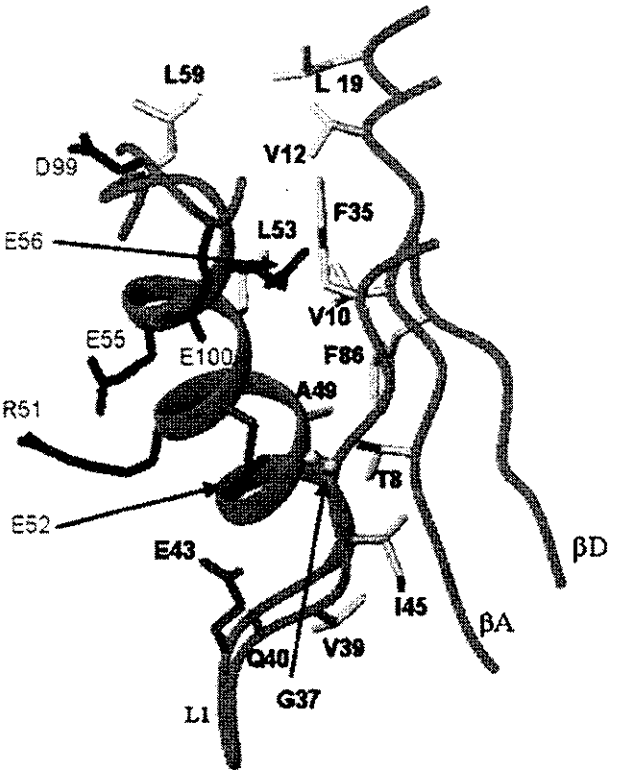

FIG. 3. **The Nudix motif of MTH1.** Exposed residues of the MTH1 Nudix motif that are conserved in other family members, Arg^{51}, Glu^{52}, Glu^{55}, Glu^{56}, Asp^{99}, and Glu^{100}, are shown in *red*. Of these, Asp^{99} and Glu^{100} are putative metal-coordinating residues. The conserved Gly^{37} residue, which is essential for catalytic activity, is shown in *gray*. The hydrophobic residues, which mediate contacts with those from strands βA and βD, and loop 1, are shown in *yellow*. Glu^{43} and Gln^{40}, which form a hydrogen bond that is important for the hairpin structure (see text), are shown in *green*.

The nucleotide-binding pocket in MTH1 suggested by the chemical shift perturbation experiments is juxtaposed to exposed residues from the Nudix motif, such as Arg^{51}, Glu^{52}, Glu^{55}, and Glu^{56} (Fig. 5*B* and Fig. 6*A*). MutT has a hydrophobic cleft at the same position, which has been shown to serve as the base-binding site in structures of its complex with a nonhydrolyzable analog, AMPCPP, and with 8-oxo-dGMP (54), a product of the hydrolysis reaction (Fig. 6*C*). Our chemical shift perturbation experiments and the structural similarity of MTH1 and MutT suggest that the pocket of MTH1 acts as the binding site for the base moiety of ligand nucleotides. In contrast, the Nudix motif of MTH1 probably binds to phosphate groups of the substrate indirectly via coordinated metals, as seen in the MutT-AMPCPP complex (55). The position of the Nudix motif relative to the nucleotide-binding pocket is similar in MutT and MTH1.

Although MTH1 and MutT seem to possess the base-binding pocket at the same position on the protein surface, their shapes are dissimilar, as shown in Fig. 6, *A* and *B*. The pocket in MTH1 is much deeper and narrower because of the presence in part of the pocket wall defined by residues Phe^{27}, Asn^{33}, Trp^{117}, and Asp^{119} from loop L1 or L4 (Fig. 6, *A* and *B*). These residues on one side form the pocket on the other side and make contact with residues from the β-hairpin, comprised of strand βF-loop-strand βG, which is missing in MutT (Fig. 4*B*). Therefore, the different shape of the MTH1 pocket can be attributed, at least partly, to the presence of the hairpin segment.